

Fig. 4.68 Mean bubble departure diameters for various coolant mass fluxes for stable saturated flow boiling (a) and various imposed heat fluxes for transient saturated flow boiling for  $G=300\pm 5\% \text{ kg/m}^2\text{s}$  with  $t_p=10 \text{ sec}$  (b), 20sec (c) and 30 sec (d).

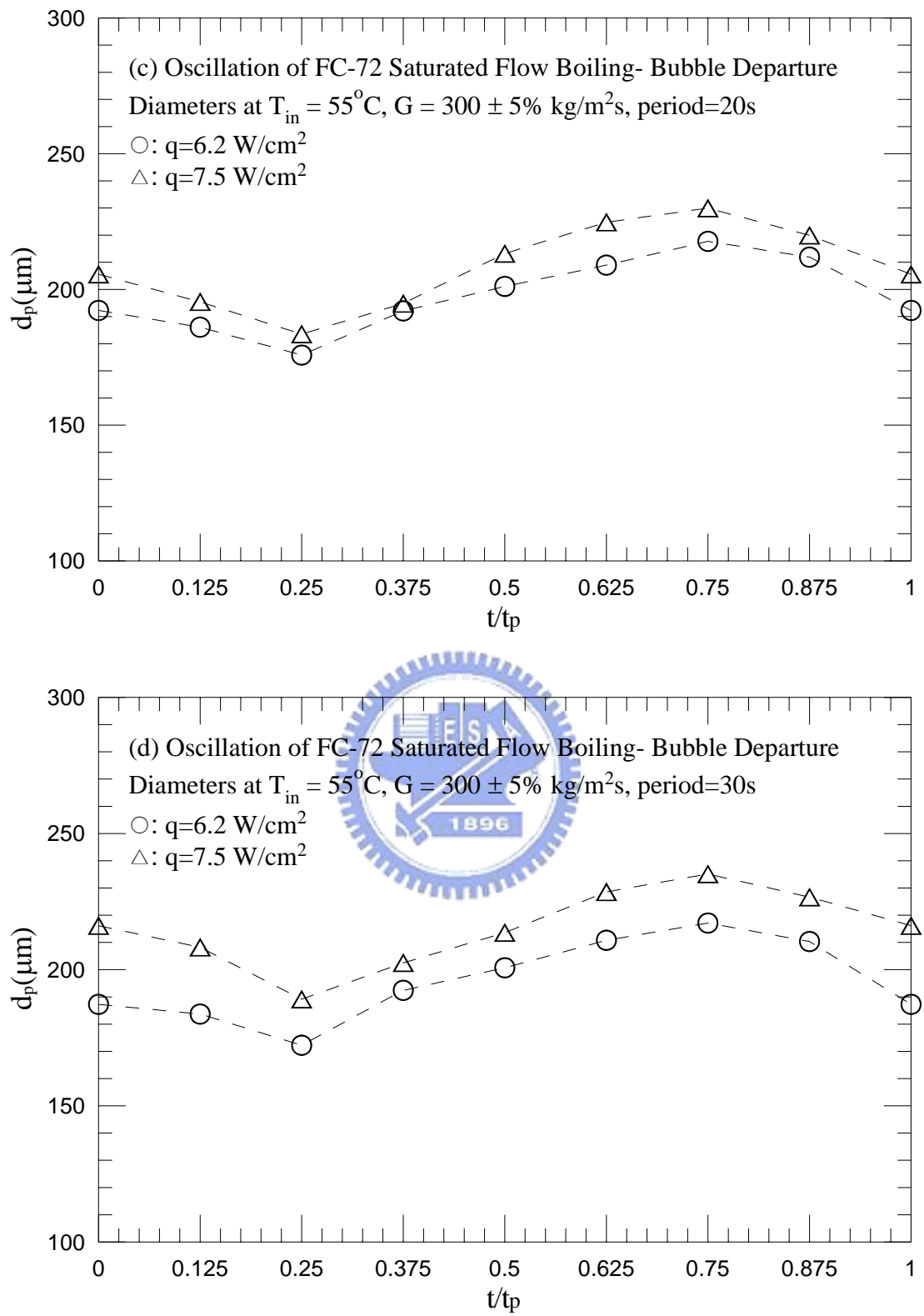


Fig. 4.68 Continued.

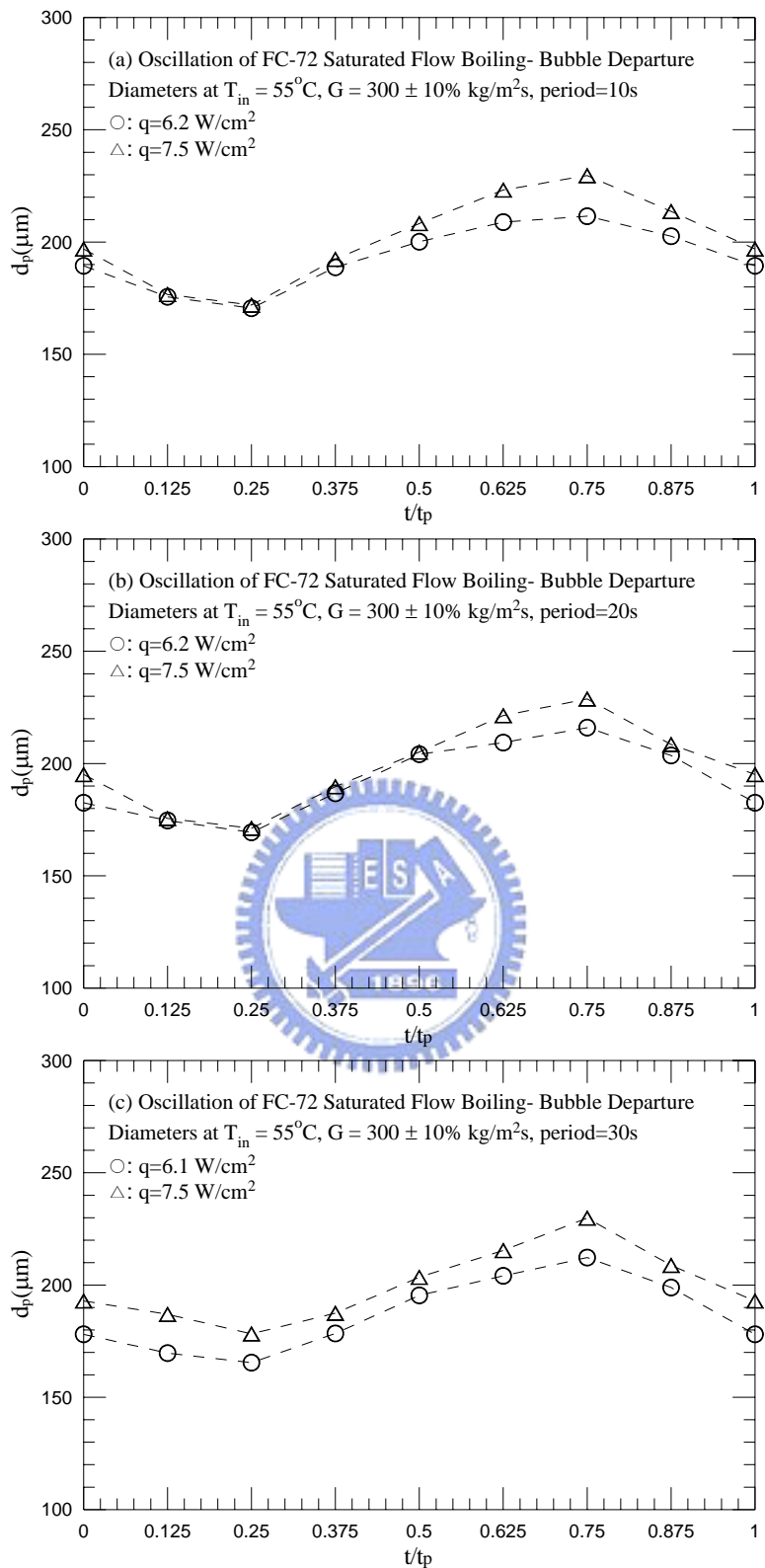


Fig. 4.69 Mean bubble departure diameters for various imposed heat fluxes for transient saturated flow boiling for  $G=300\pm10\% \text{ kg/m}^2\text{s}$  with  $t_p=10 \text{ sec}$  (a),  $20\text{sec}$  (b) and  $30 \text{ sec}$  (c).

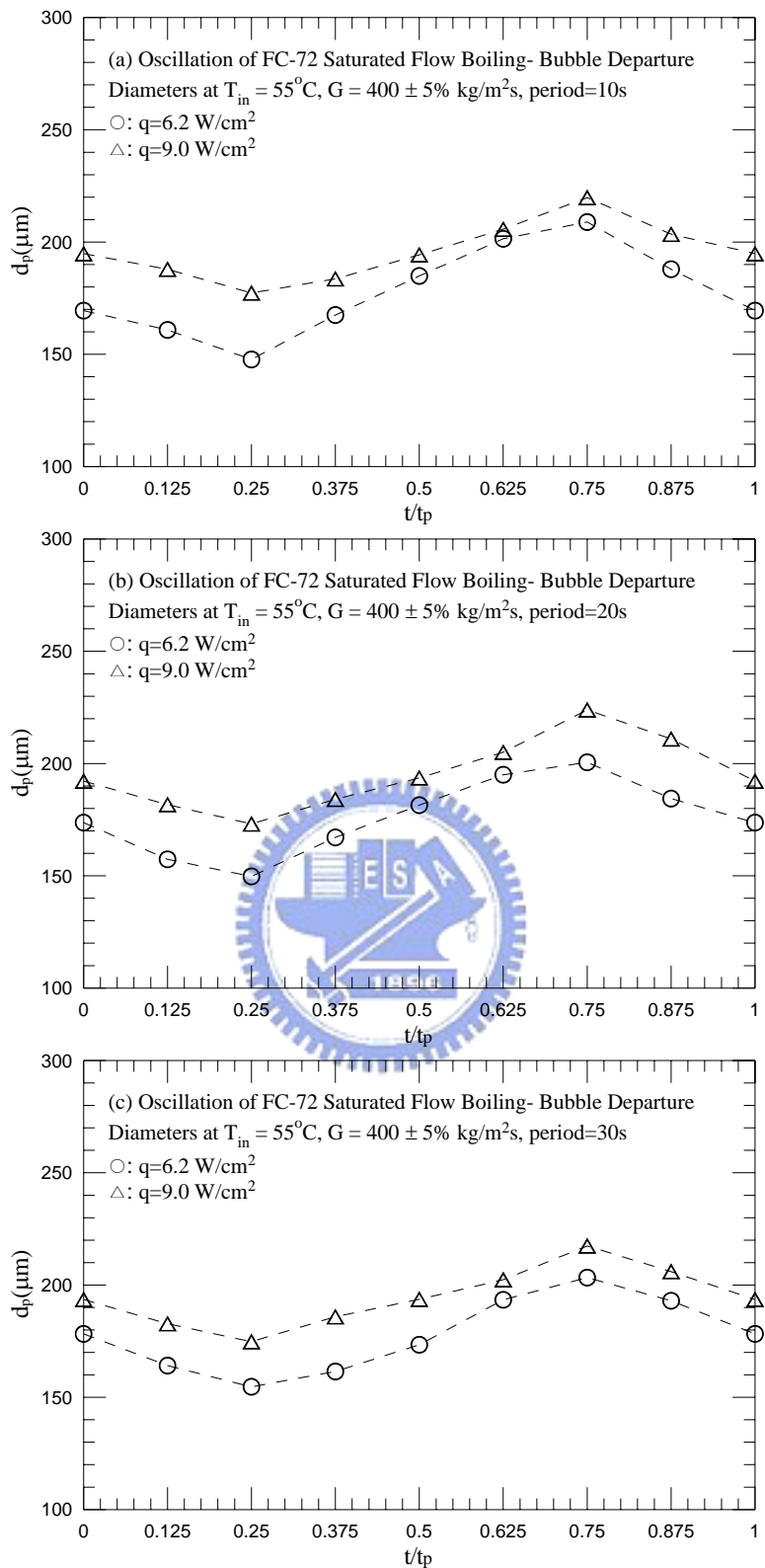


Fig. 4.70 Mean bubble departure diameters for various imposed heat fluxes for transient saturated flow boiling for  $G=400 \pm 5\% \text{ kg/m}^2\text{s}$  with  $t_p=10 \text{ sec}$  (a),  $20 \text{ sec}$  (b) and  $30 \text{ sec}$  (c).

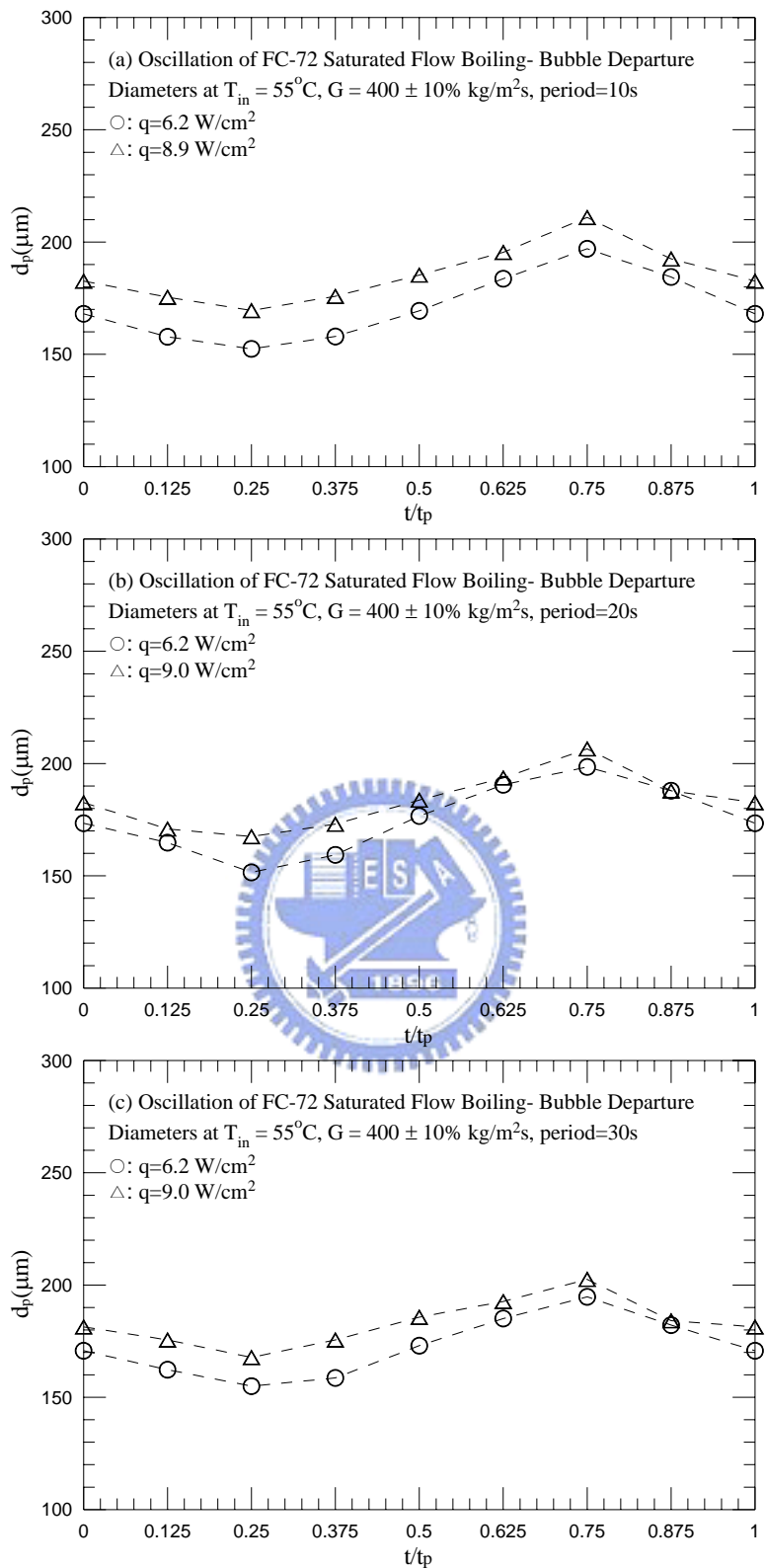


Fig. 4.71 Mean bubble departure diameters for various imposed heat fluxes for transient saturated flow boiling for  $G=400\pm10\% \text{ kg/m}^2\text{s}$  with  $t_p=10 \text{ sec}$  (a),  $20\text{sec}$  (b) and  $30 \text{ sec}$  (c).

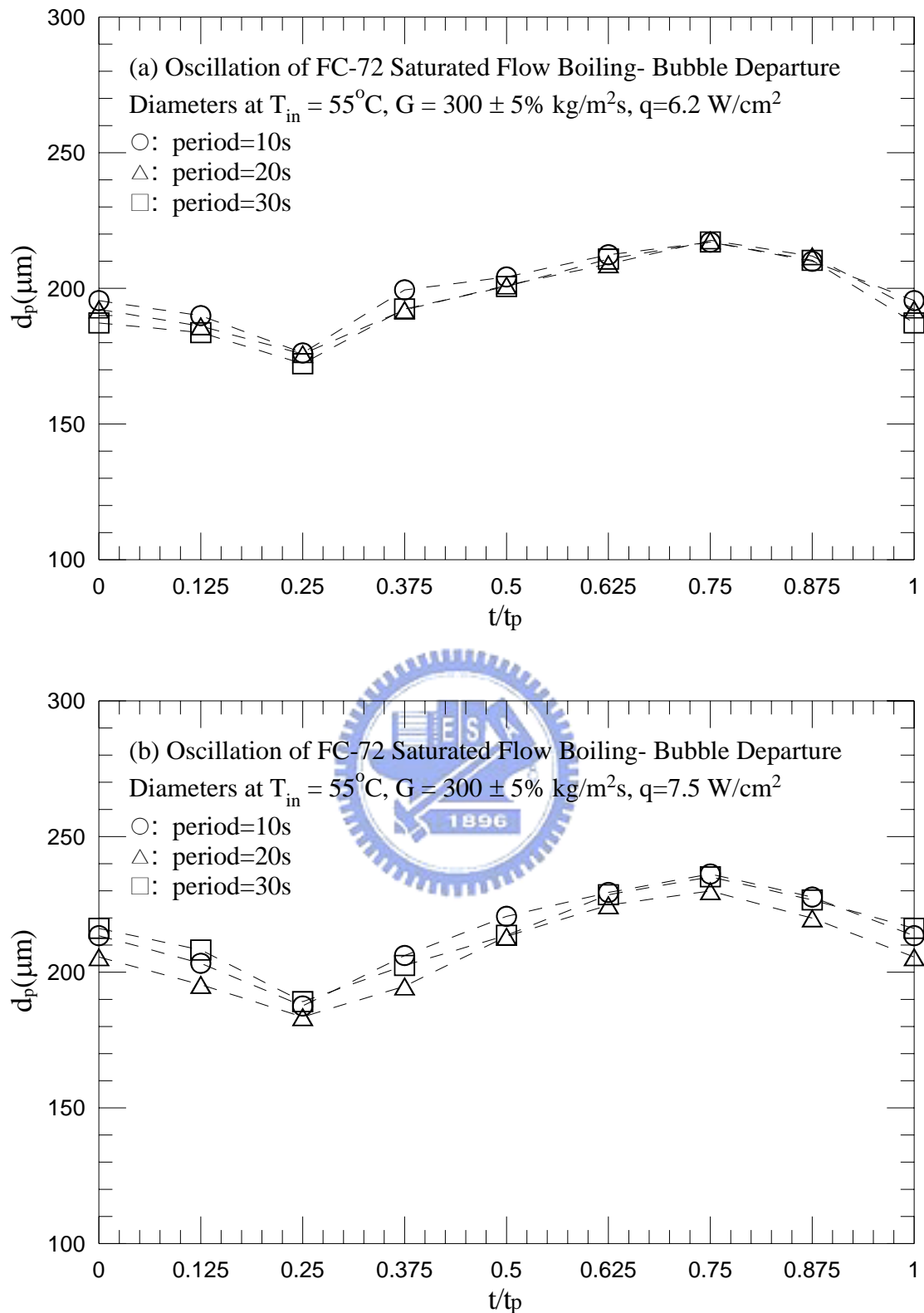


Fig. 4.72 Mean bubble departure diameters for various periods of the mass flux oscillation for transient saturated flow boiling for  $G=300\pm 5\% \text{ kg/m}^2\text{s}$  with (a)  $q=6.2 \text{ W/cm}^2$  and (b)  $q=7.5 \text{ W/cm}^2$ .

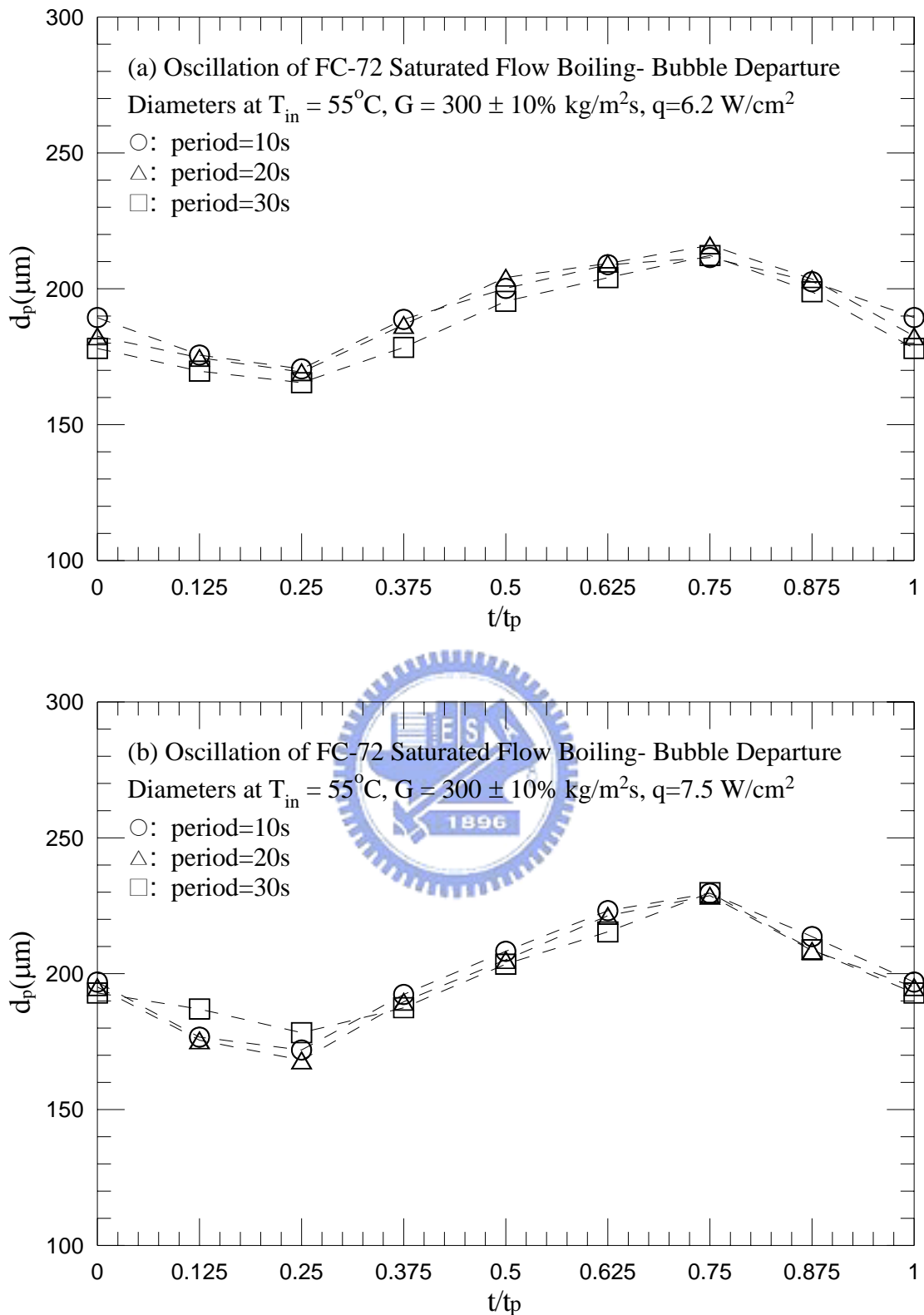


Fig. 4.73 Mean bubble departure diameters for various periods of the mass flux oscillation for transient saturated flow boiling for  $G=300\pm10\% \text{ kg/m}^2\text{s}$  with (a)  $q=6.2 \text{ W/cm}^2$  and (b)  $q=7.5 \text{ W/cm}^2$ .

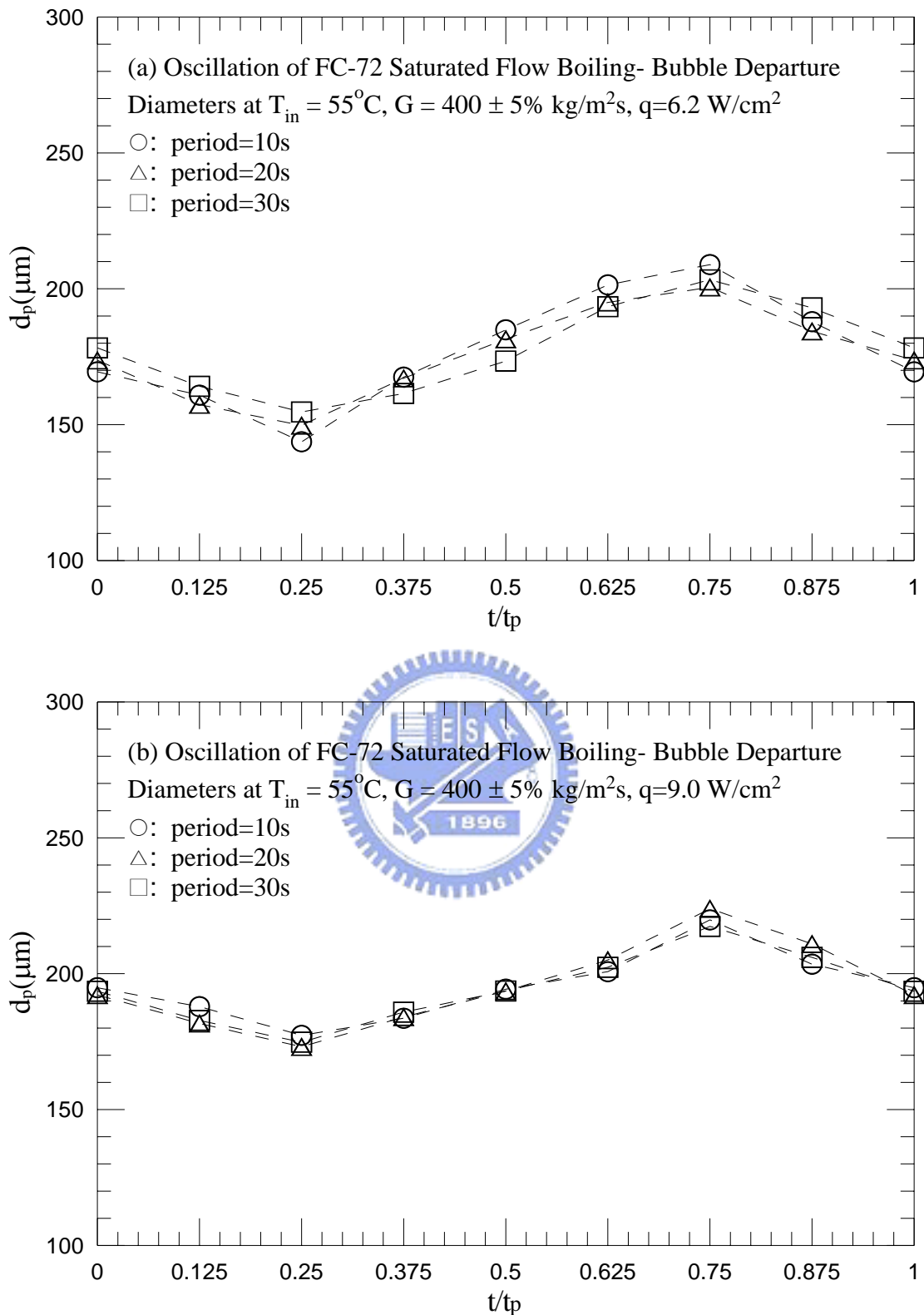


Fig. 4.74 Mean bubble departure diameters for various periods of the mass flux oscillation for transient saturated flow boiling for  $G=400\pm 5\% \text{ kg/m}^2\text{s}$  with (a)  $q=6.2 \text{ W/cm}^2$  and (b)  $q=9.0 \text{ W/cm}^2$ .

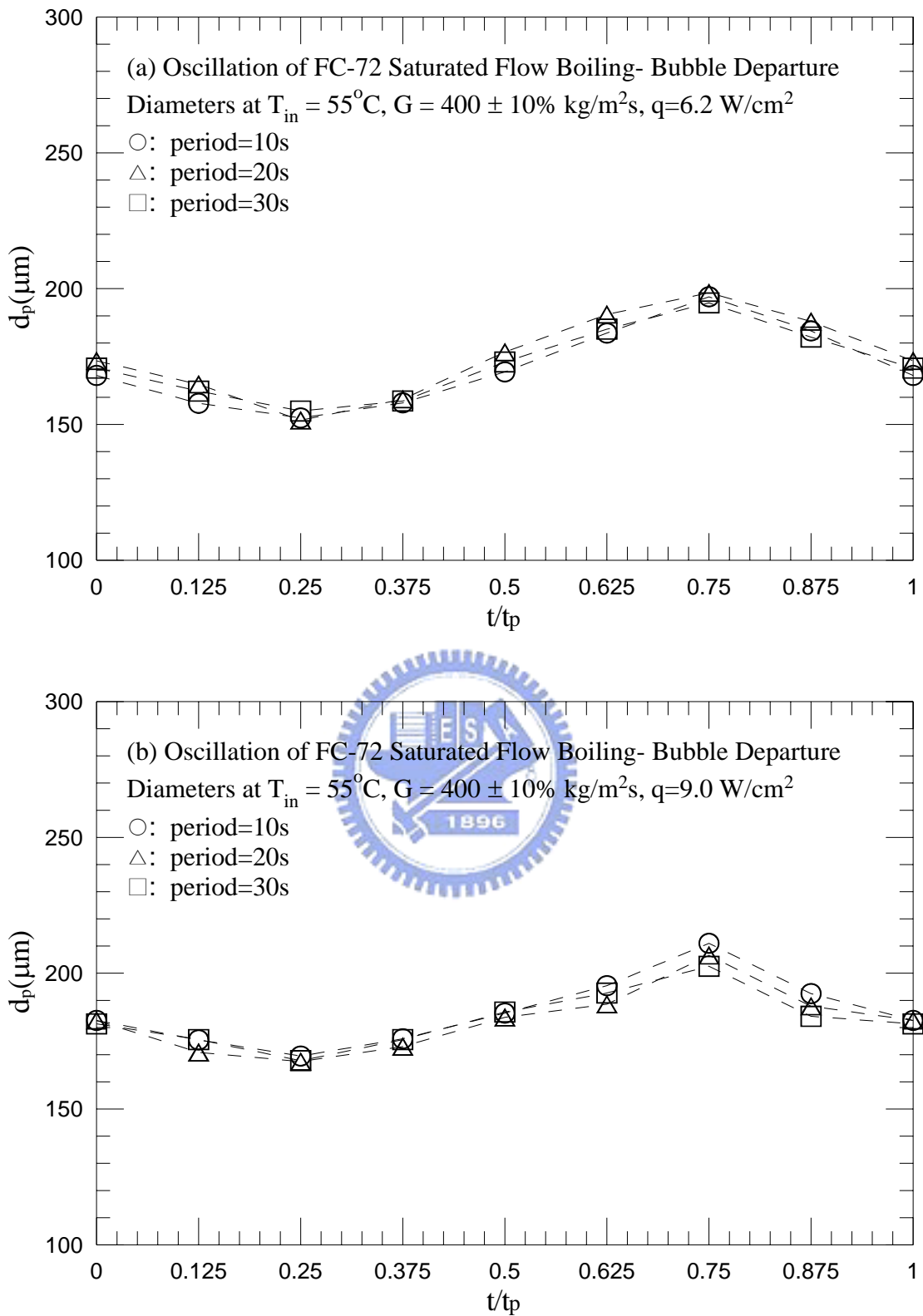


Fig. 4.75 Mean bubble departure diameters for various periods of the mass flux oscillation for transient saturated flow boiling for  $G=400\pm10\% \text{ kg/m}^2\text{s}$  with (a)  $q=6.2 \text{ W/cm}^2$  and (b)  $q=9.0 \text{ W/cm}^2$ .

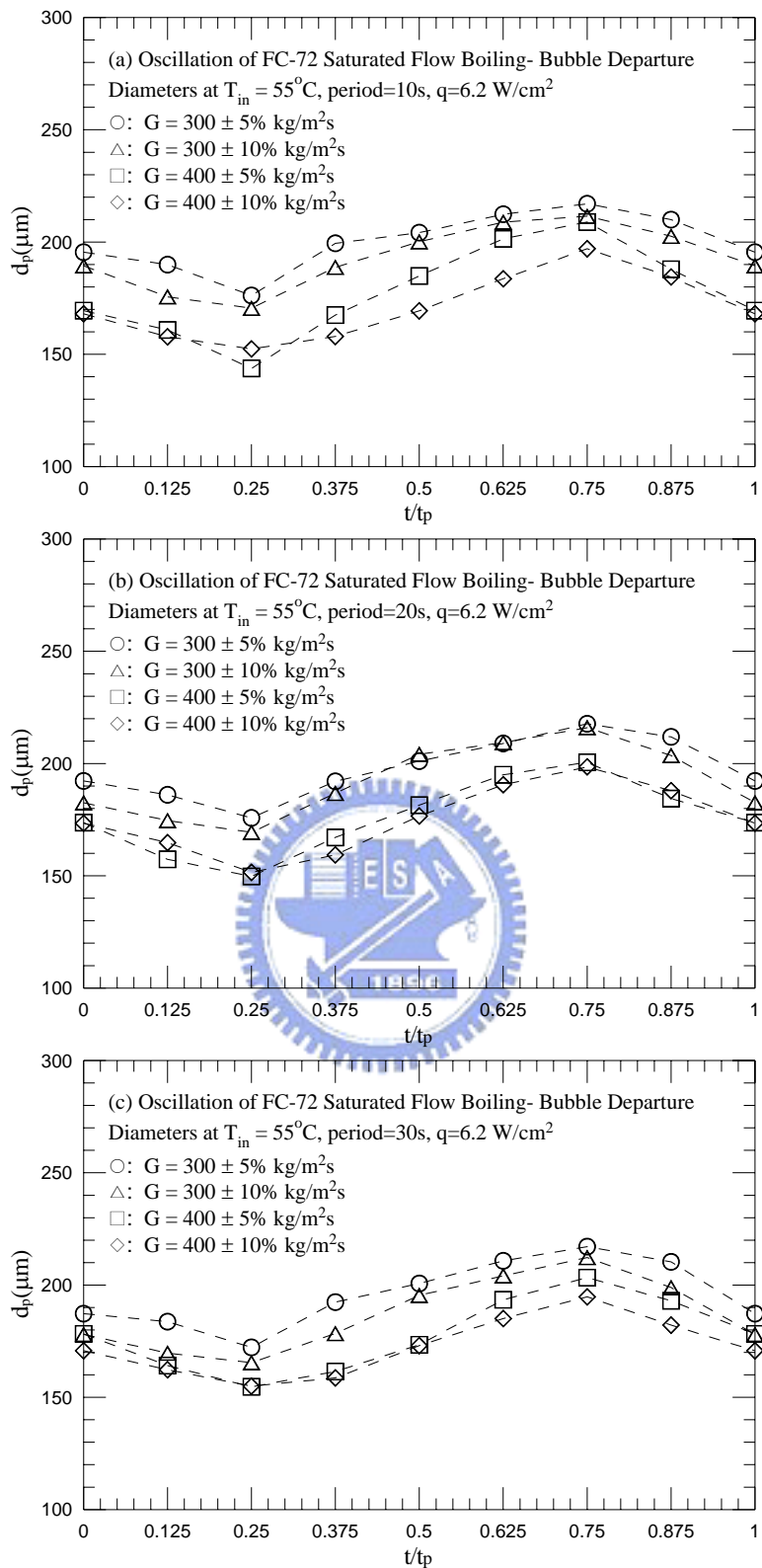


Fig. 4.76 Mean bubble departure diameters for various amplitudes of the mass fluxes oscillation for transient saturated flow boiling for  $q=6.2 \text{ W/cm}^2$  with period=10 sec (a), 20 sec (b), and 30 sec (c).

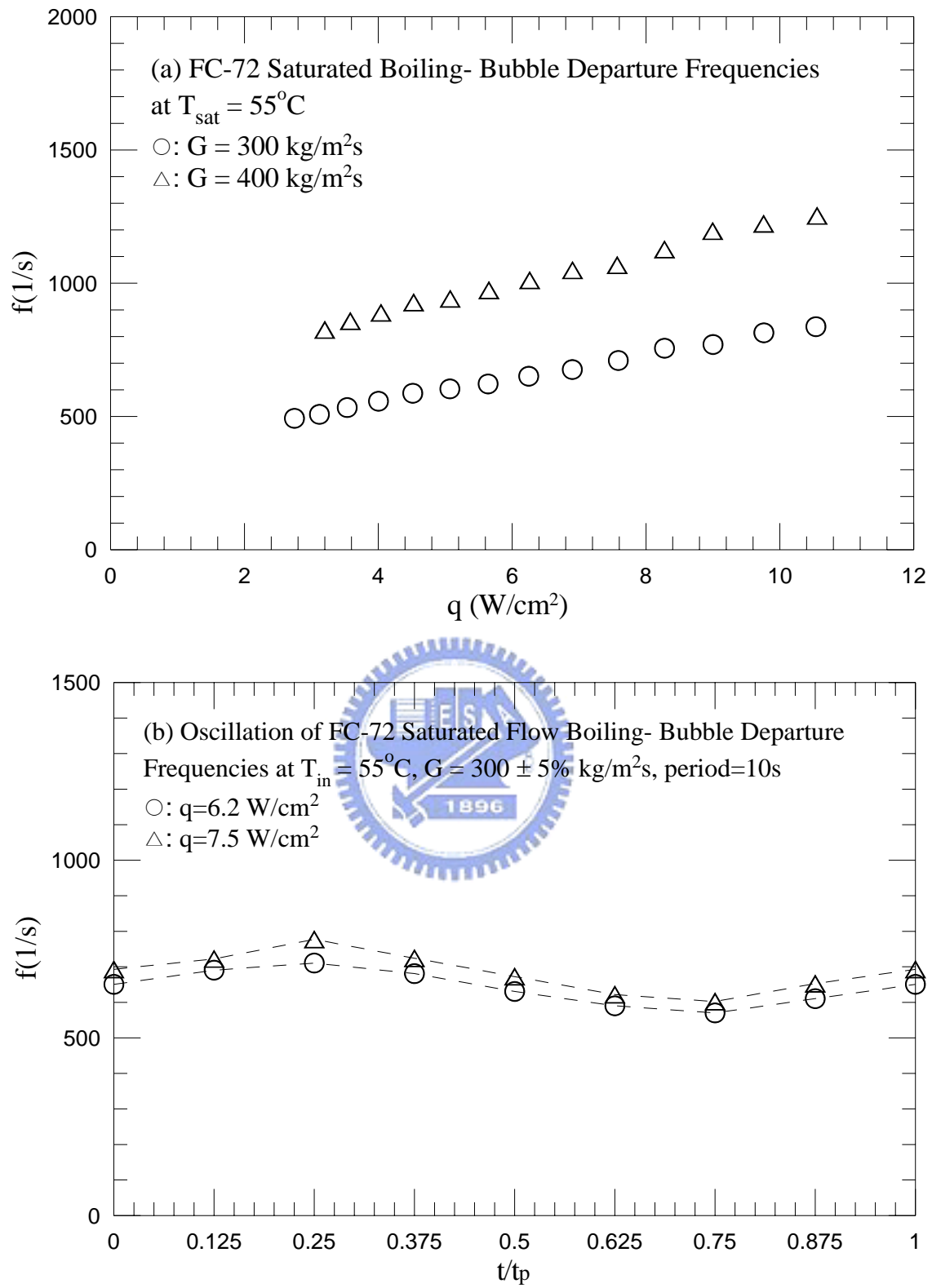


Fig. 4.77 Mean bubble departure frequencies for various coolant mass fluxes for stable saturated flow boiling (a) and various imposed heat fluxes for transient saturated flow boiling for  $G=300\pm 5\% \text{ kg/m}^2\text{s}$  with  $t_p=10 \text{ sec}$  (b), 20sec (c) and 30 sec (d).

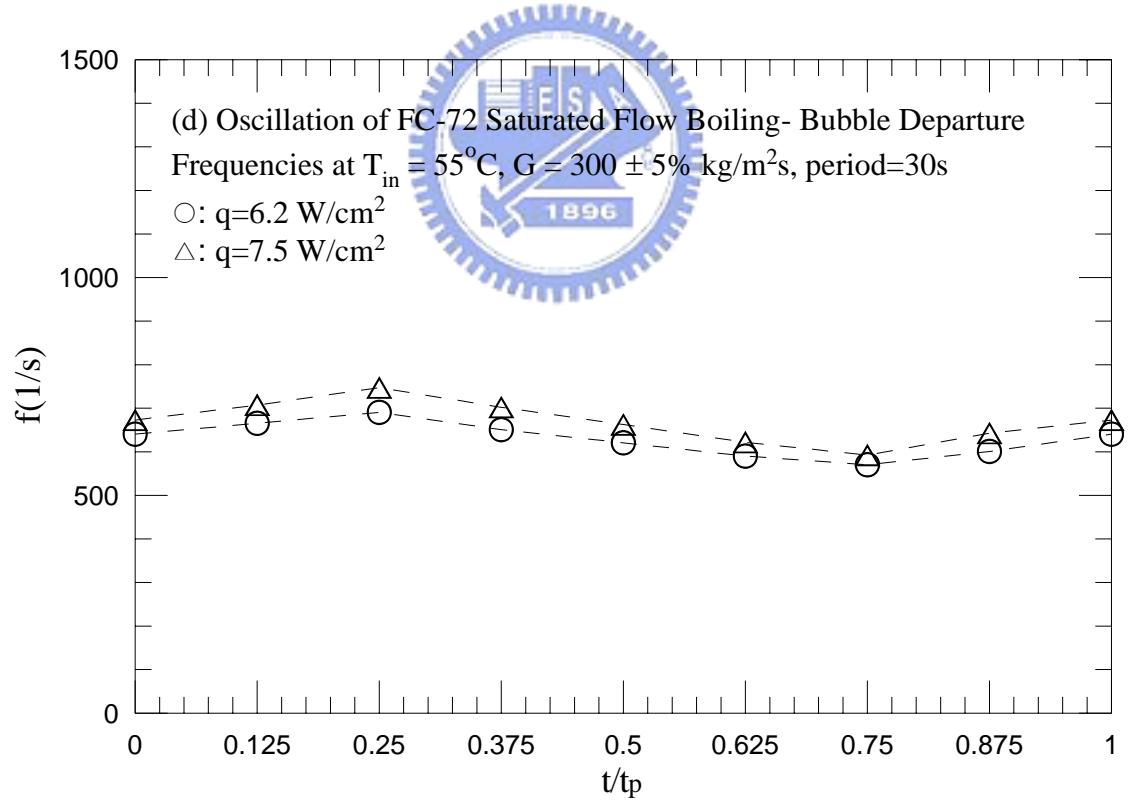
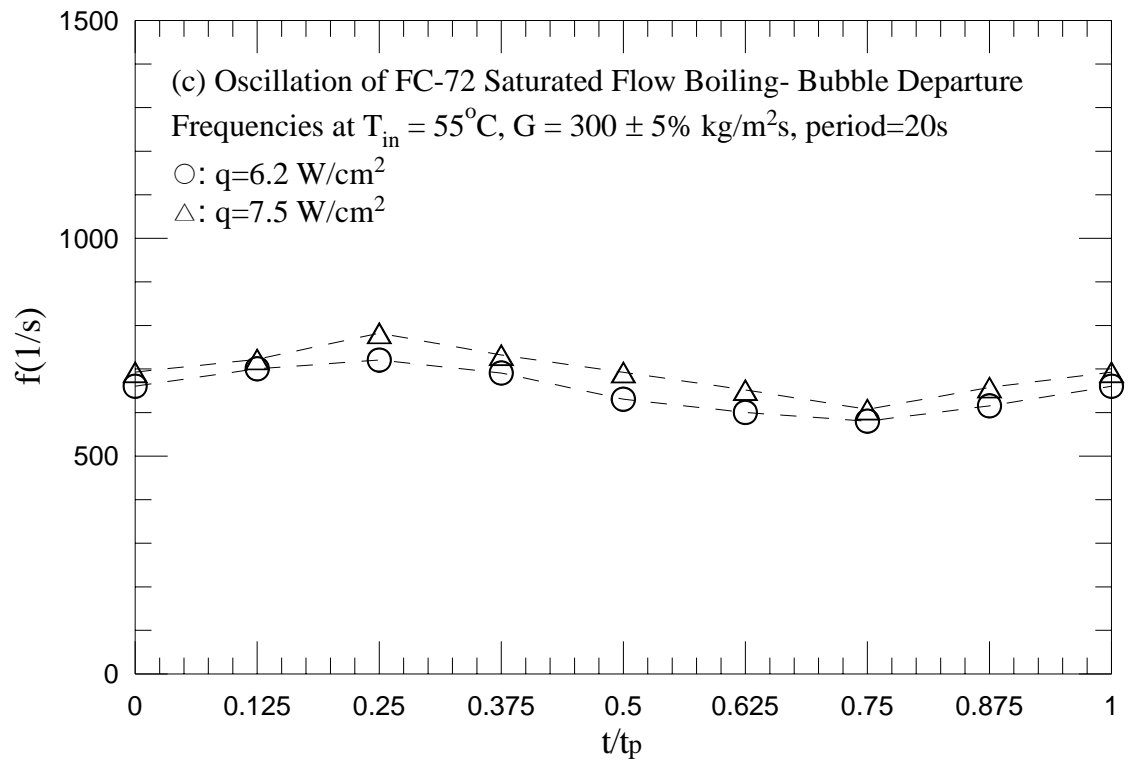


Fig. 4.77 Continued.

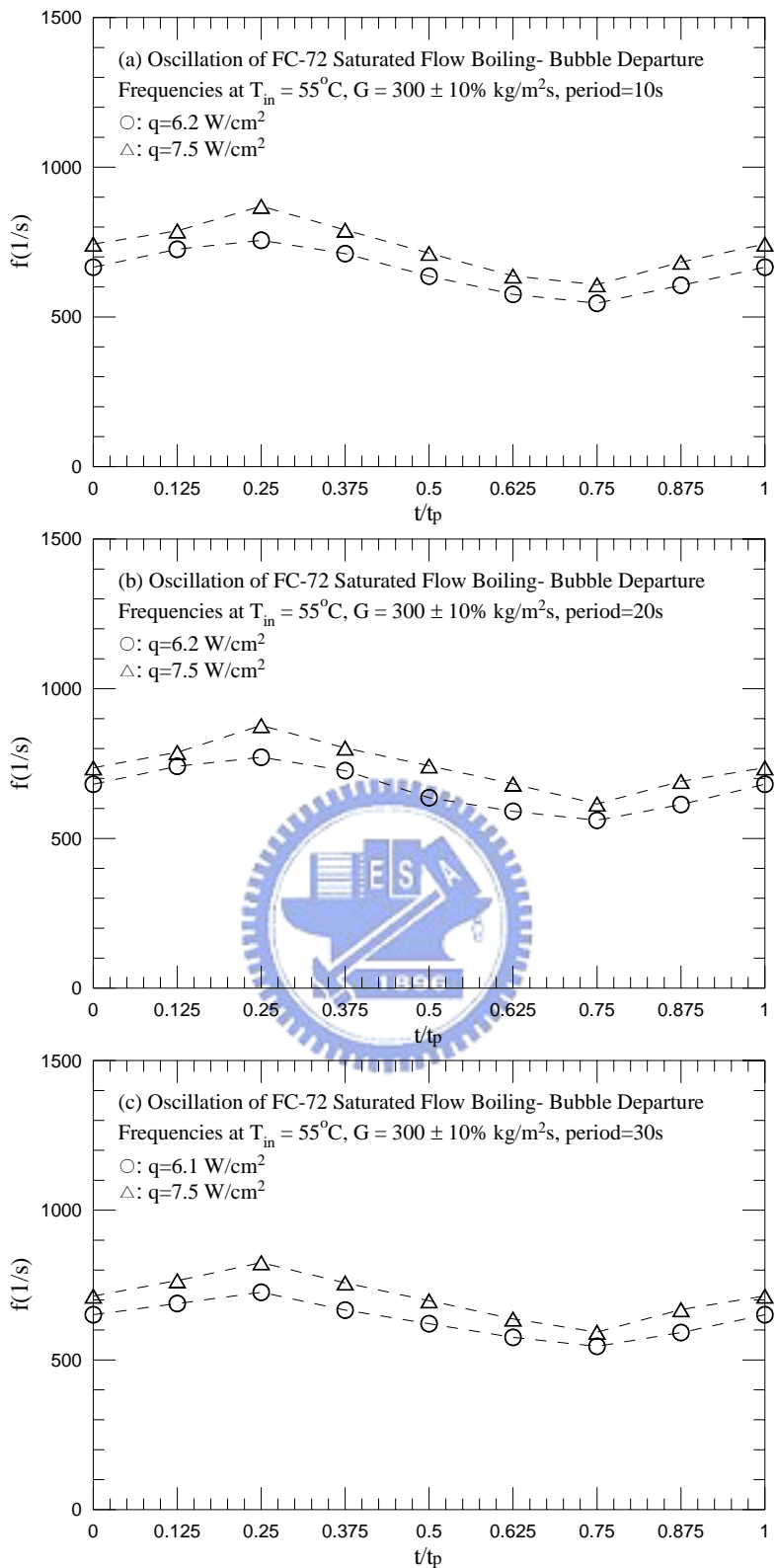


Fig. 4.78 Mean bubble departure frequencies for various imposed heat fluxes for transient saturated flow boiling for  $G=300\pm10\% \text{ kg/m}^2\text{s}$  with  $t_p=10 \text{ sec}$  (a),  $20\text{sec}$  (b) and  $30 \text{ sec}$  (c).

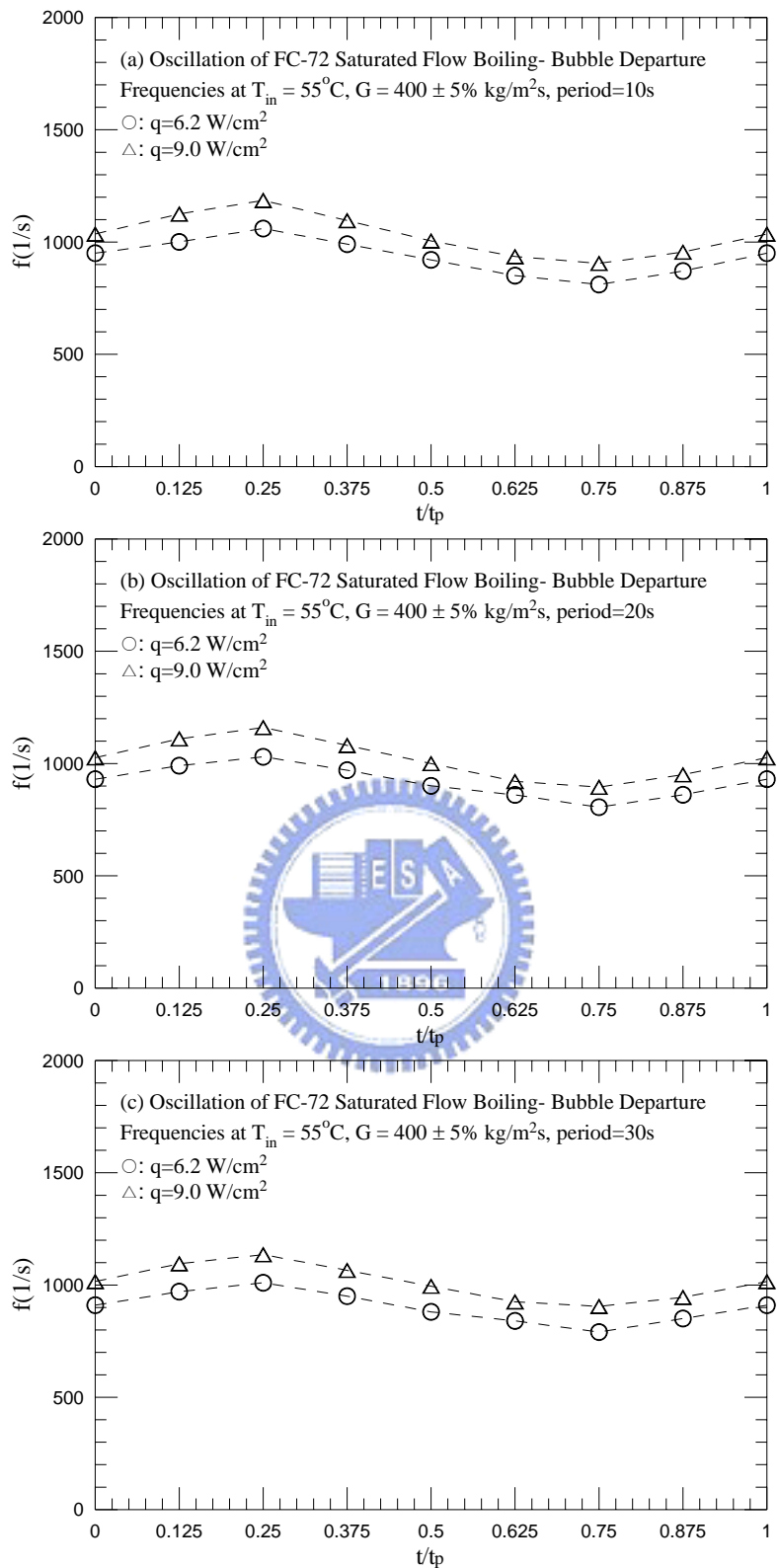


Fig. 4.79 Mean bubble departure frequencies for various imposed heat fluxes for transient saturated flow boiling for  $G=400\pm 5\% \text{ kg/m}^2\text{s}$  with  $t_p=10 \text{ sec}$  (a),  $20\text{sec}$  (b) and  $30 \text{ sec}$  (c).

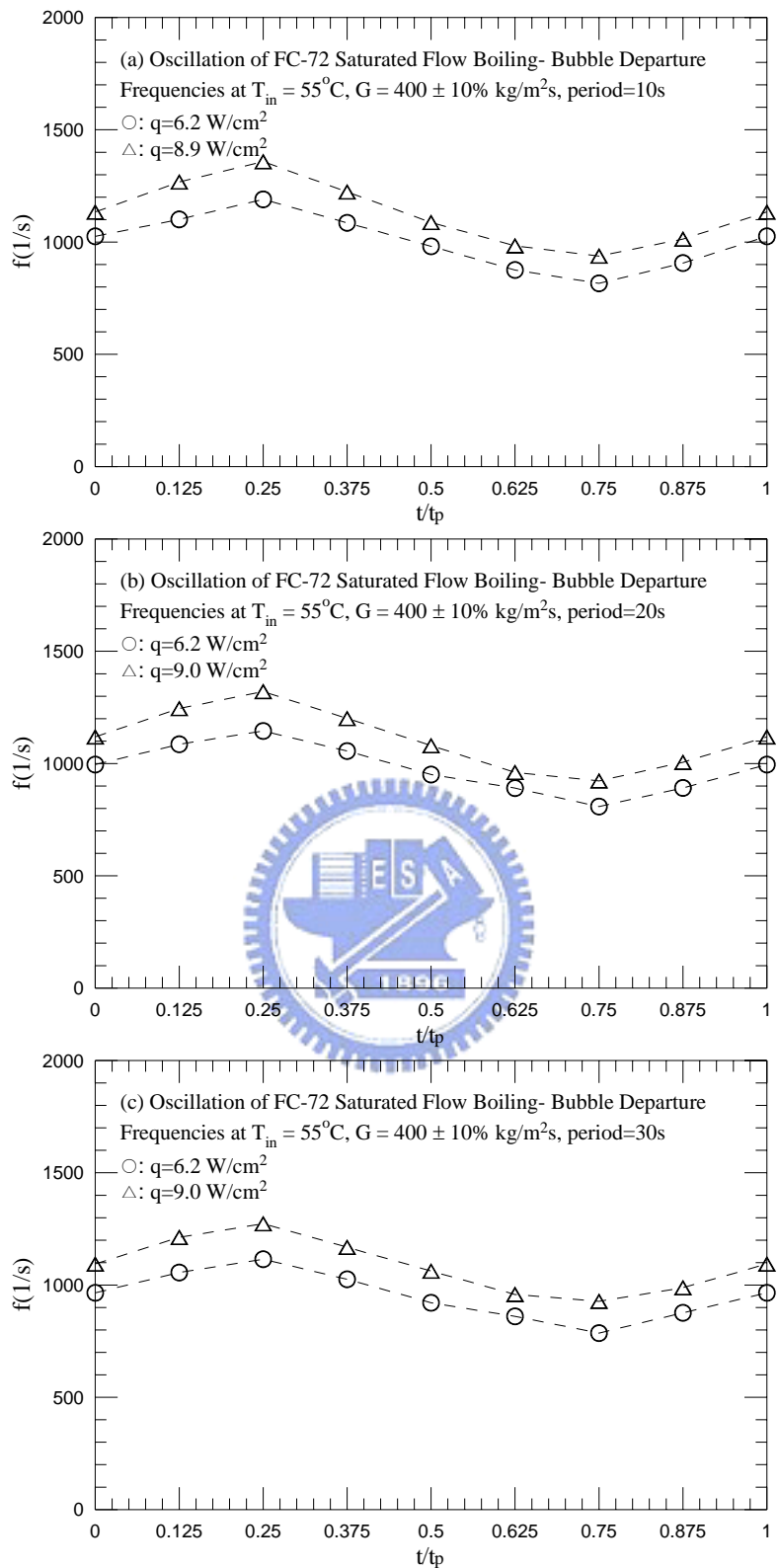


Fig. 4.80 Mean bubble departure frequencies for various imposed heat fluxes for transient saturated flow boiling for  $G=400\pm10\% \text{ kg/m}^2\text{s}$  with  $t_p=10 \text{ sec}$  (a),  $20\text{sec}$  (b) and  $30 \text{ sec}$  (c).

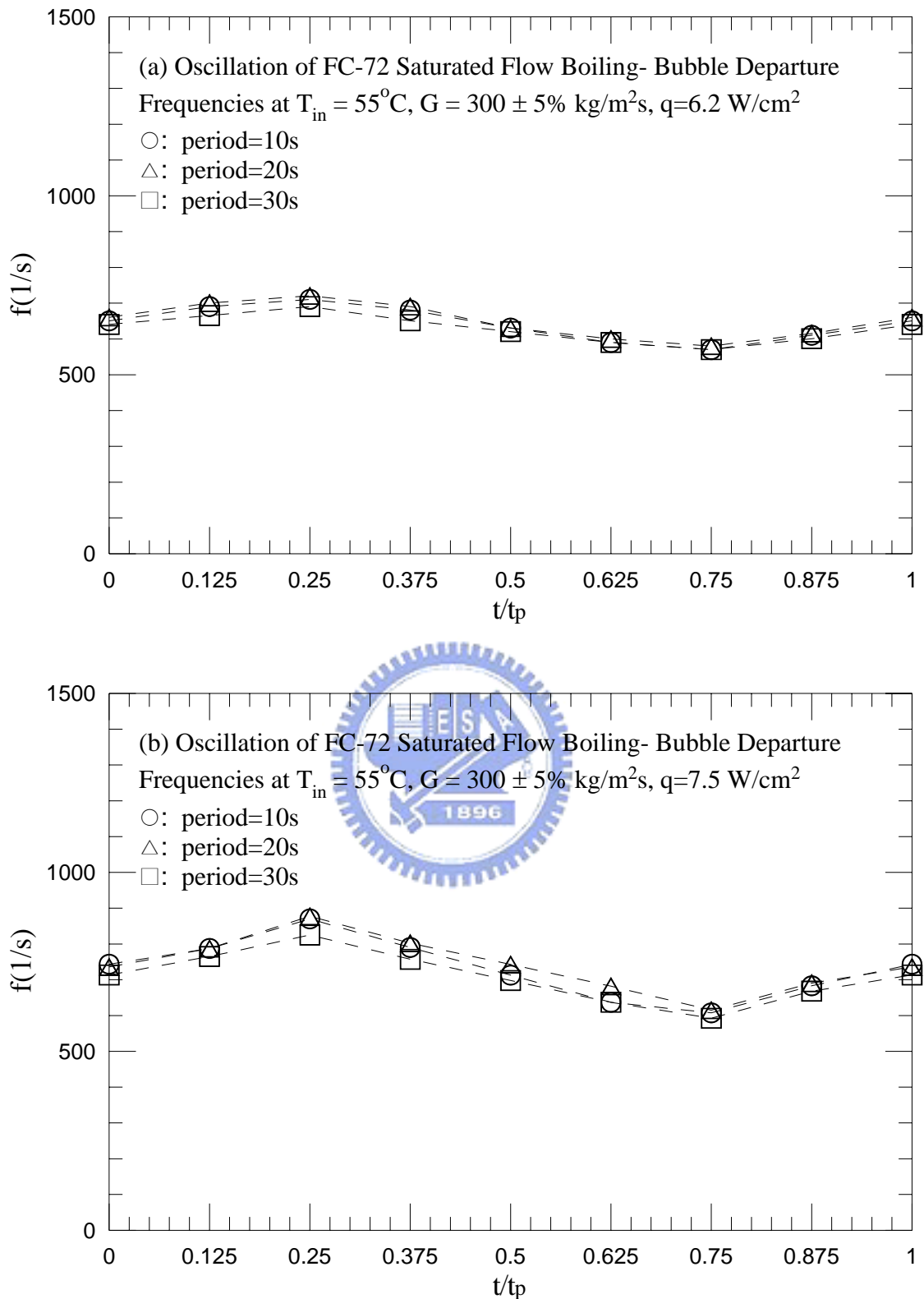


Fig. 4.81 Mean bubble departure frequencies for various periods of mass flux oscillation for transient saturated flow boiling for  $G=300\pm 5\% \text{ kg/m}^2\text{s}$  with (a)  $q=6.2 \text{ W/cm}^2$  and (b)  $q=7.5 \text{ W/cm}^2$ .

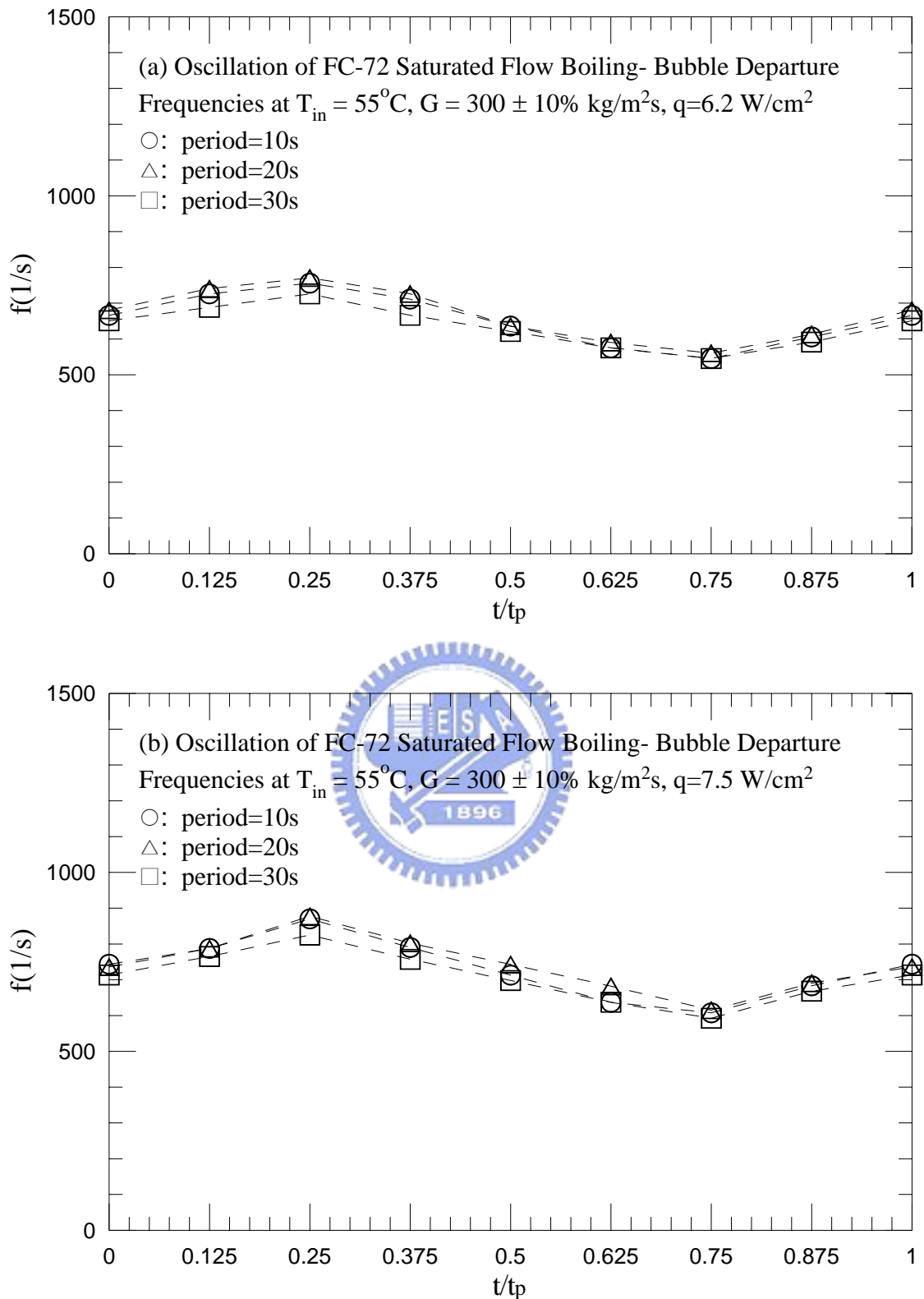


Fig. 4.82 Mean bubble departure frequencies for various periods of mass flux oscillation for transient saturated flow boiling for  $G=300\pm10\% \text{ kg/m}^2\text{s}$  with (a)  $q=6.2 \text{ W/cm}^2$  and (b)  $q=7.5 \text{ W/cm}^2$ .

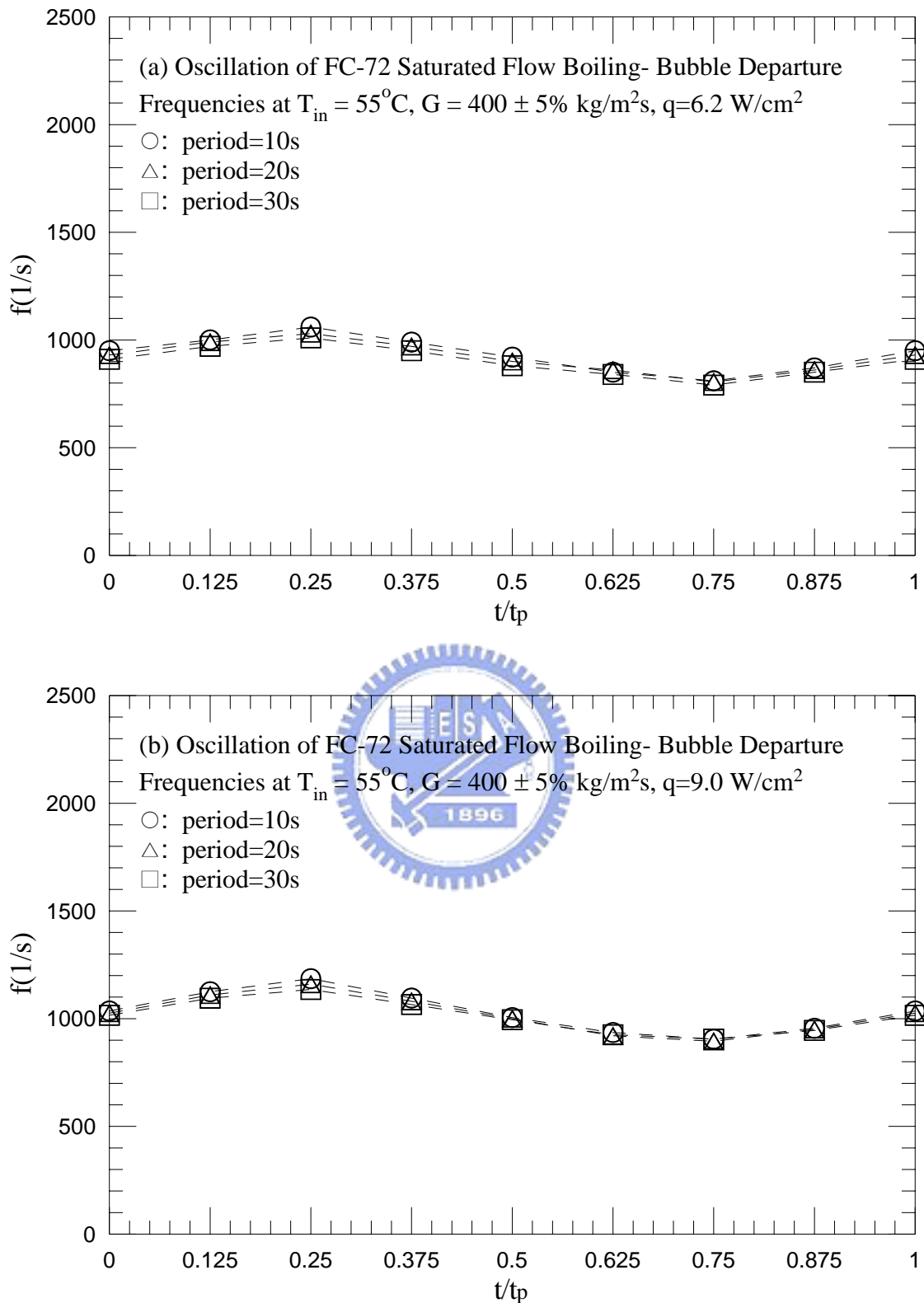


Fig. 4.83 Mean bubble departure frequencies for various periods of mass flux oscillation for transient saturated flow boiling for  $G=400\pm 5\% \text{ kg/m}^2\text{s}$  with (a)  $q=6.2 \text{ W/cm}^2$  and (b)  $q=9.0 \text{ W/cm}^2$ .

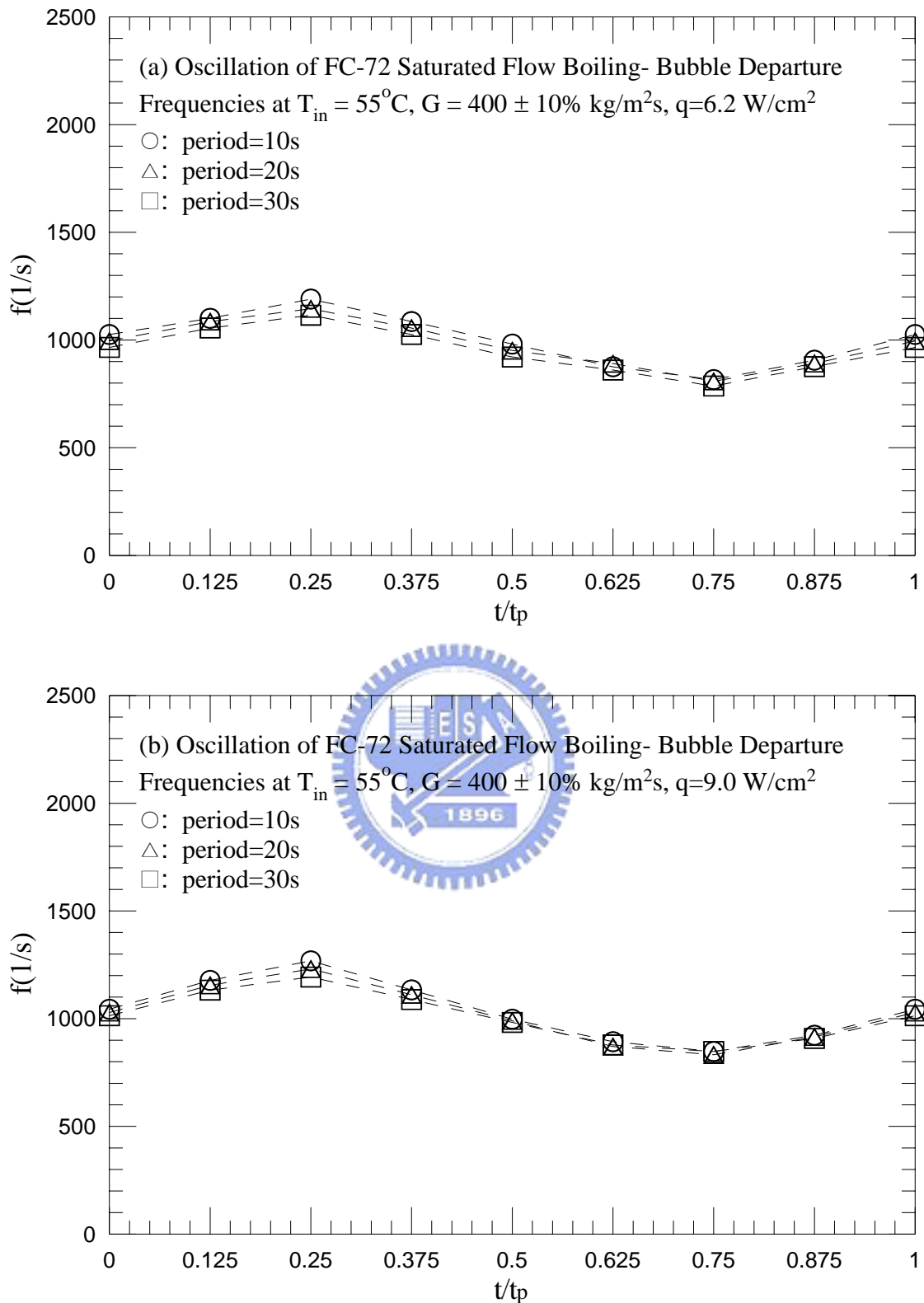


Fig. 4.84 Mean bubble departure frequencies for various periods of mass flux oscillation for transient saturated flow boiling for  $G=400 \pm 10\% \text{ kg/m}^2\text{s}$  with (a)  $q=6.2 \text{ W/cm}^2$  and (b)  $q=9.0 \text{ W/cm}^2$ .

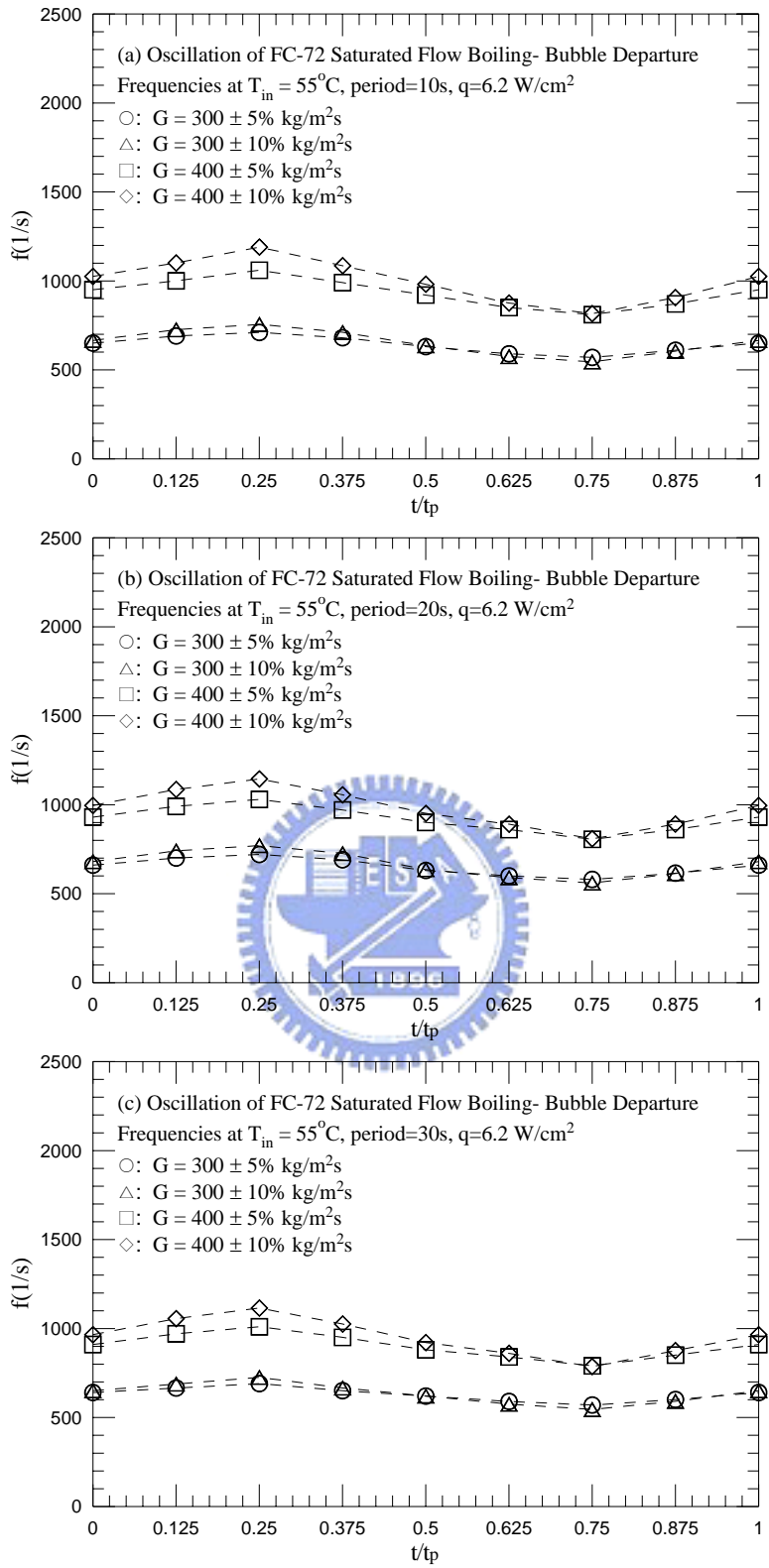


Fig. 4.85 Mean bubble departure frequencies for various amplitudes of the mass fluxes oscillation for transient saturated flow boiling for  $q=6.2 \text{ W/cm}^2$  with period=10 sec (a), 20 sec (b), and 30 sec (c).

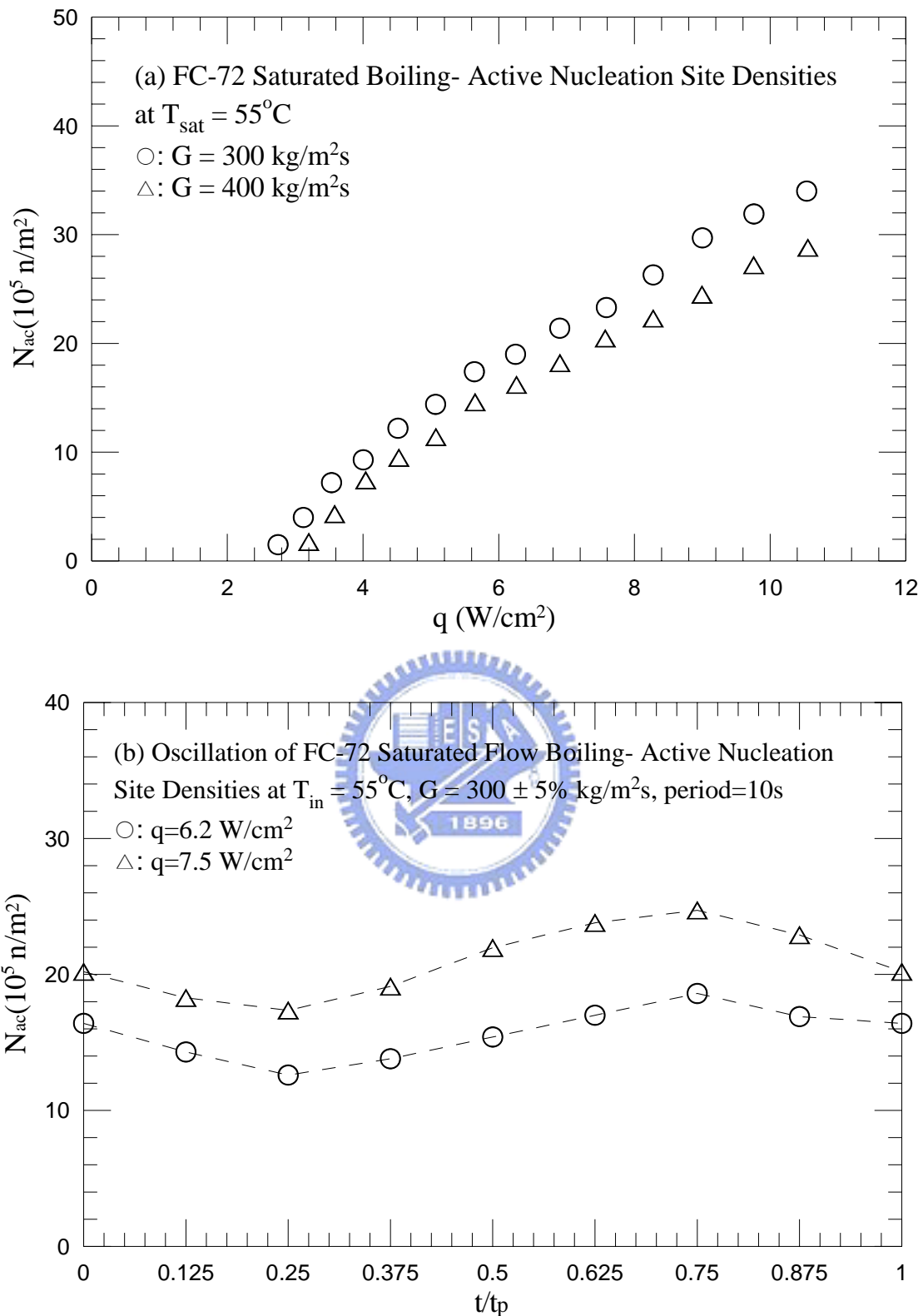


Fig. 4.86 Mean active nucleation site densities for various coolant mass fluxes for stable saturated flow boiling (a) and various imposed heat fluxes for transient saturated flow boiling for  $G=300 \pm 5\% \text{ kg/m}^2\text{s}$  with  $t_p=10 \text{ sec}$  (b),  $20 \text{ sec}$  (c) and  $30 \text{ sec}$  (d).

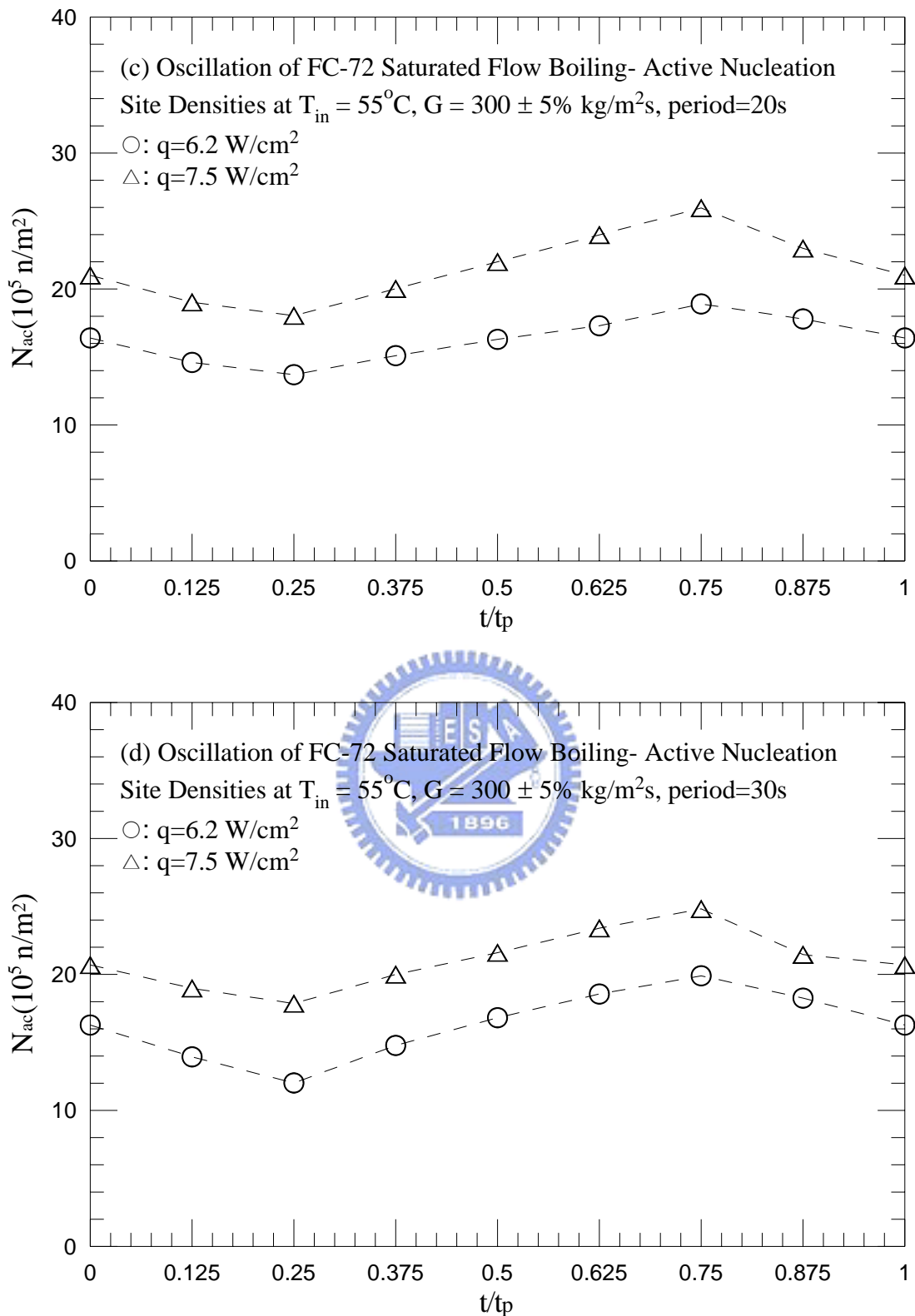


Fig. 4.86 Continued.

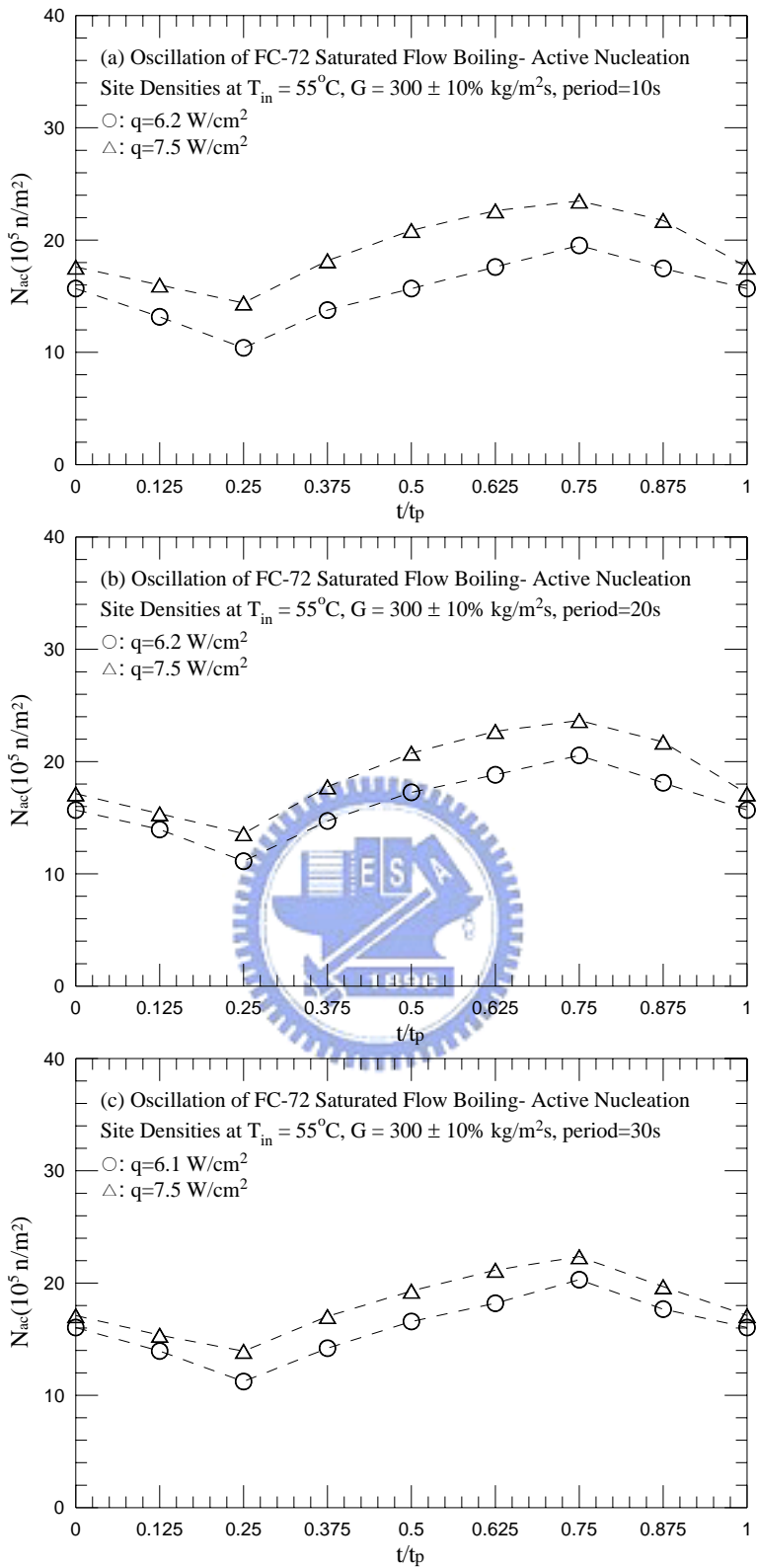


Fig. 4.87 Mean active nucleation site densities for various imposed heat fluxes for transient saturated flow boiling for  $G=300\pm10\% \text{ kg/m}^2\text{s}$  with  $t_p=10 \text{ sec}$  (a), 20sec (b) and 30 sec (c).

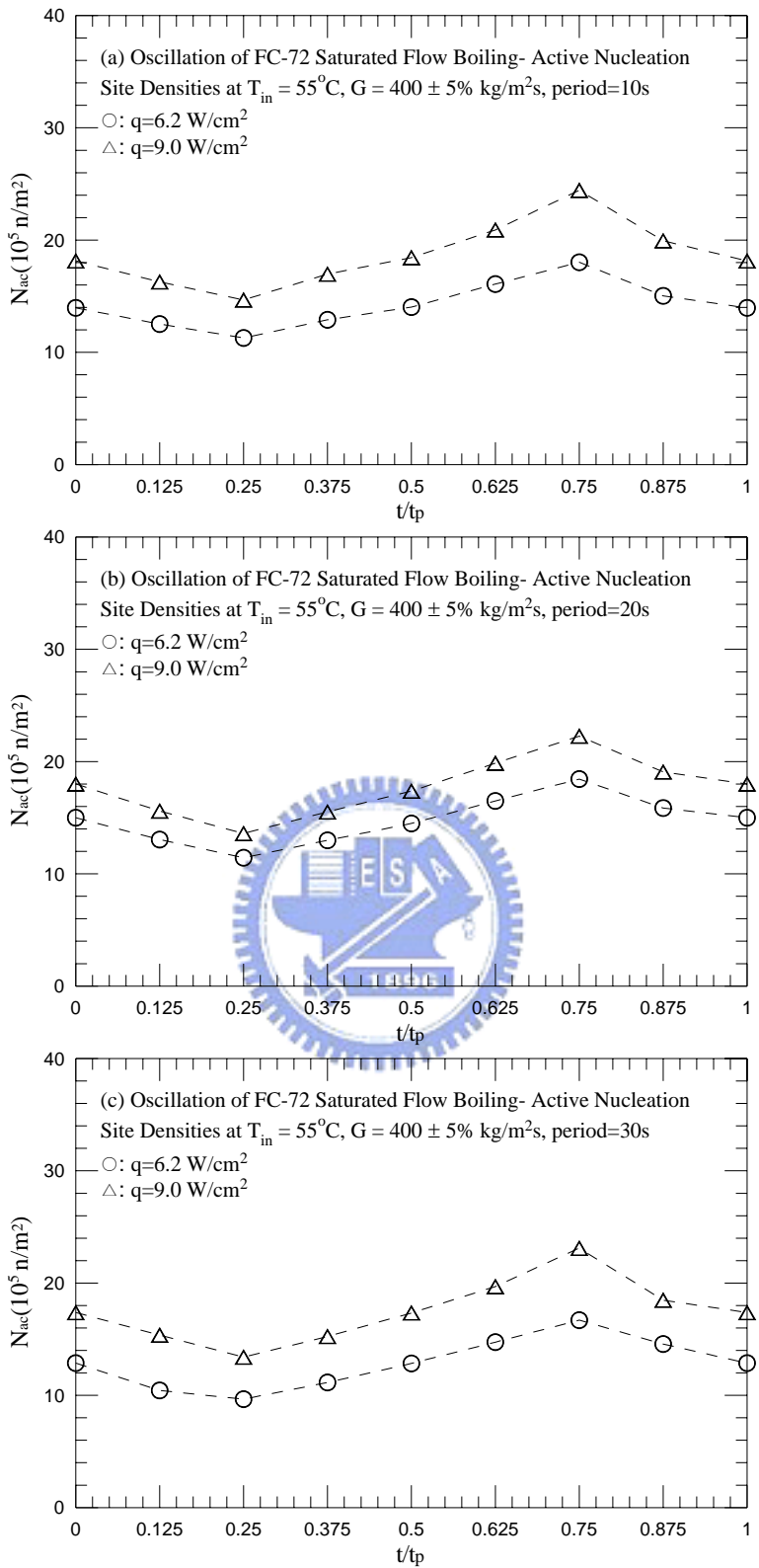


Fig. 4.88 Mean active nucleation site densities for various imposed heat fluxes for transient saturated flow boiling for  $G=400\pm5\% \text{ kg/m}^2\text{s}$  with  $t_p=10 \text{ sec}$  (a), 20sec (b) and 30 sec (c).

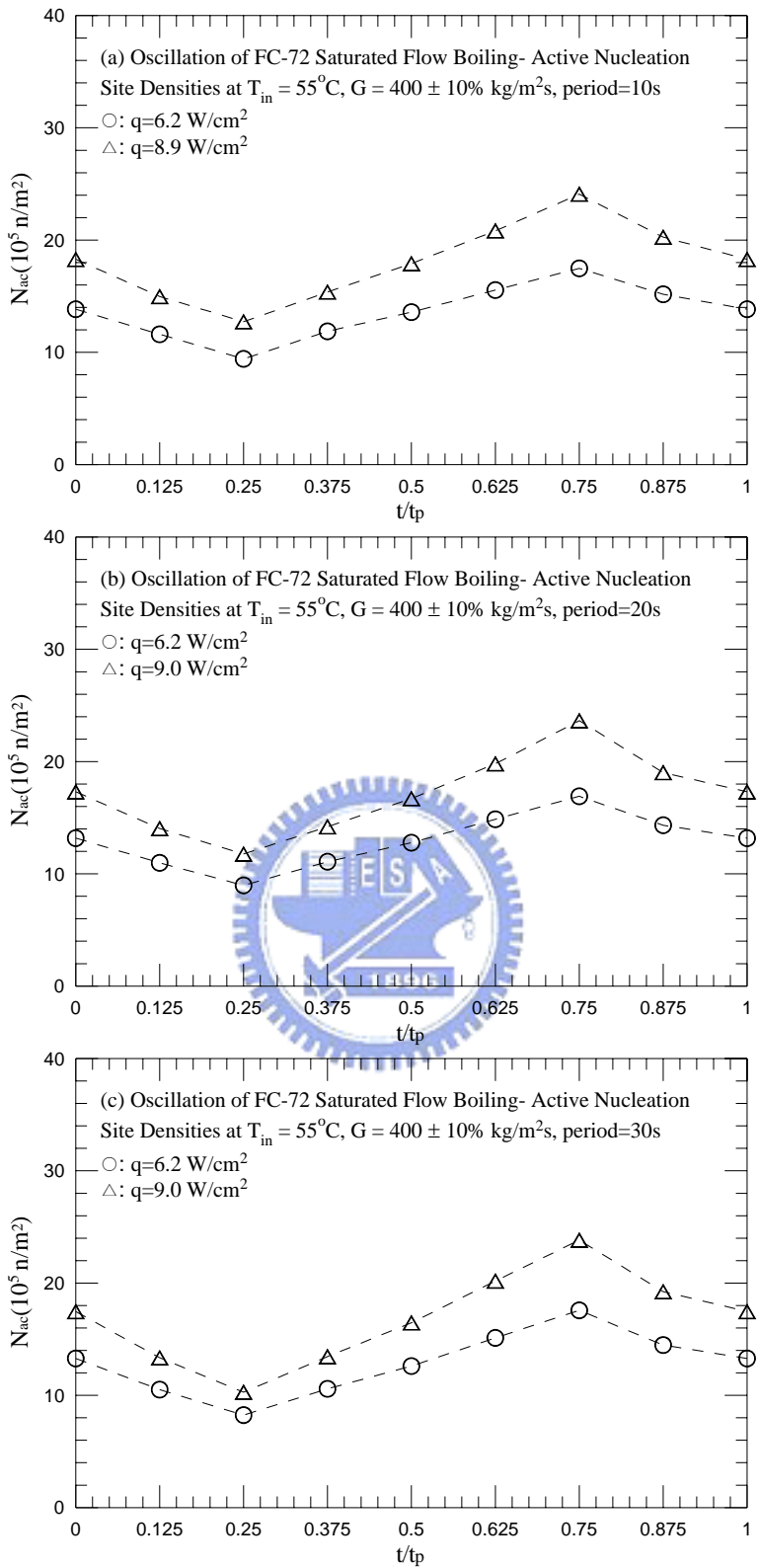


Fig. 4.89 Mean active nucleation site densities for various imposed heat fluxes for transient saturated flow boiling for  $G=400\pm10\% \text{ kg/m}^2\text{s}$  with  $t_p=10 \text{ sec}$  (a), 20sec (b) and 30 sec (c).

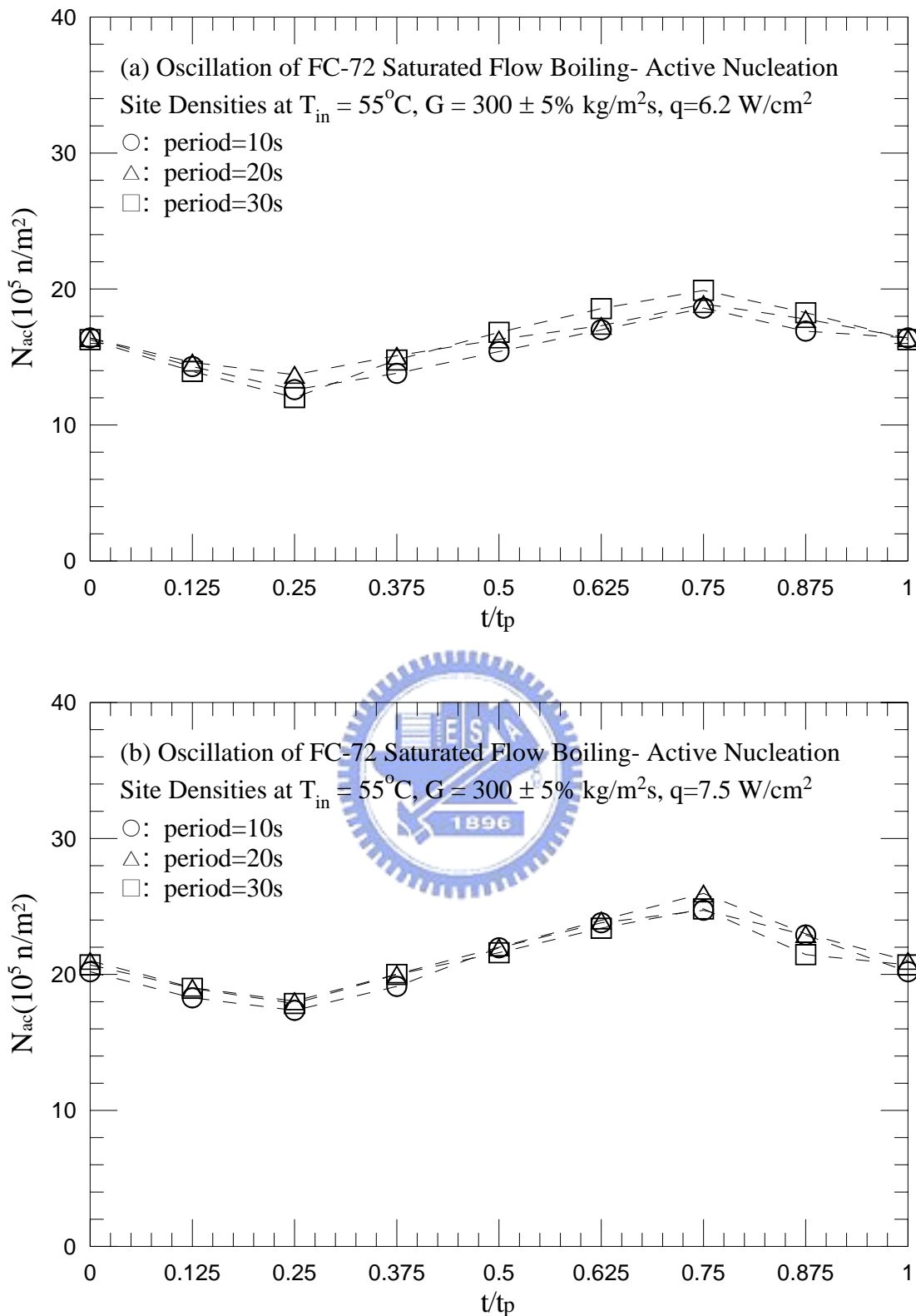


Fig. 4.90 Mean active nucleation site densities for various periods of mass flux oscillation for transient saturated flow boiling for  $G=300\pm 5\% \text{ kg/m}^2\text{s}$  with (a)  $q=6.2 \text{ W/cm}^2$  and (b)  $q=7.5 \text{ W/cm}^2$ .

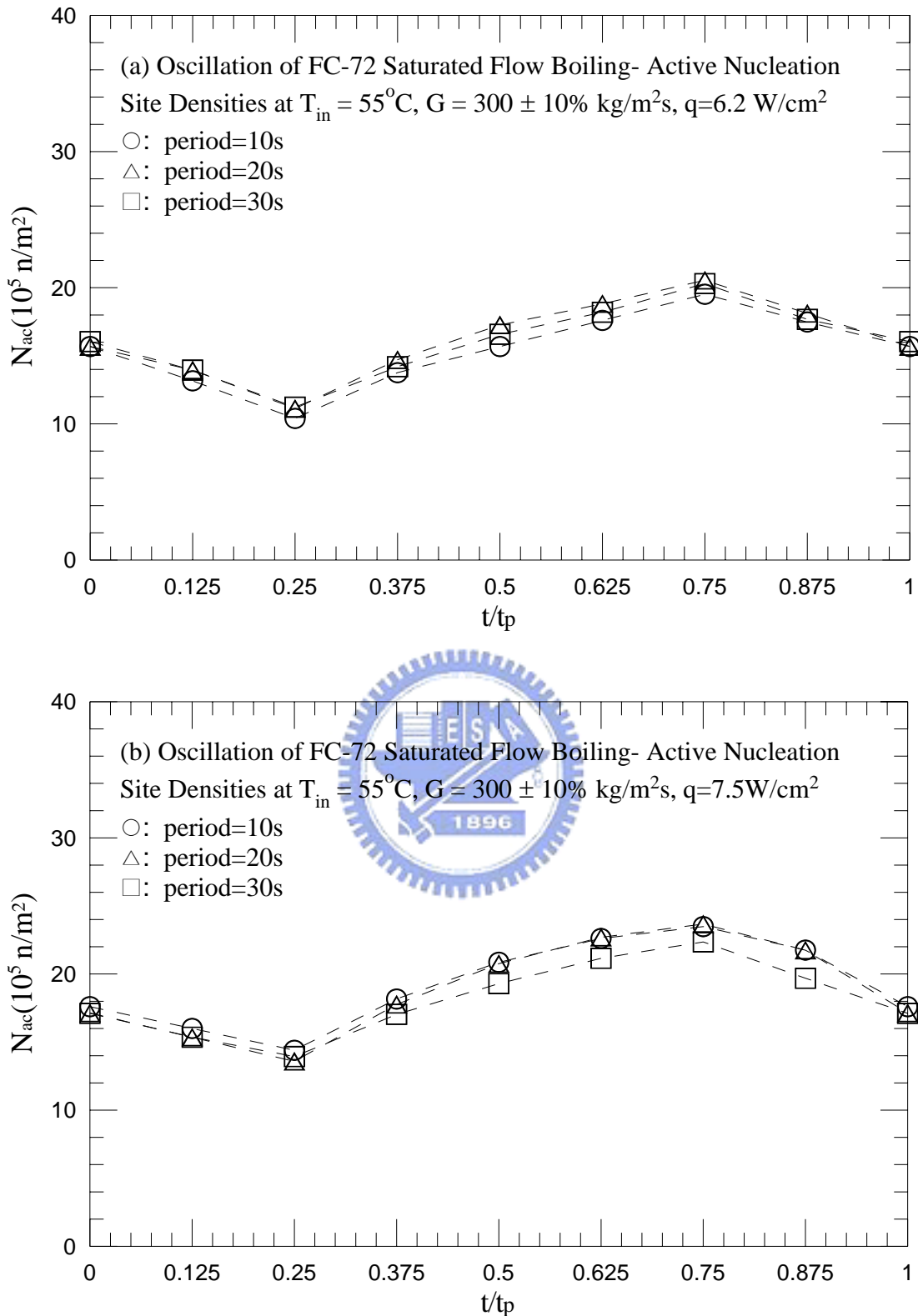


Fig. 4.91 Mean active nucleation site densities for various periods of mass flux oscillation for transient saturated flow boiling for  $G=300\pm10\% \text{ kg/m}^2\text{s}$  with (a)  $q=6.2 \text{ W/cm}^2$  and (b)  $q=7.5 \text{ W/cm}^2$ .

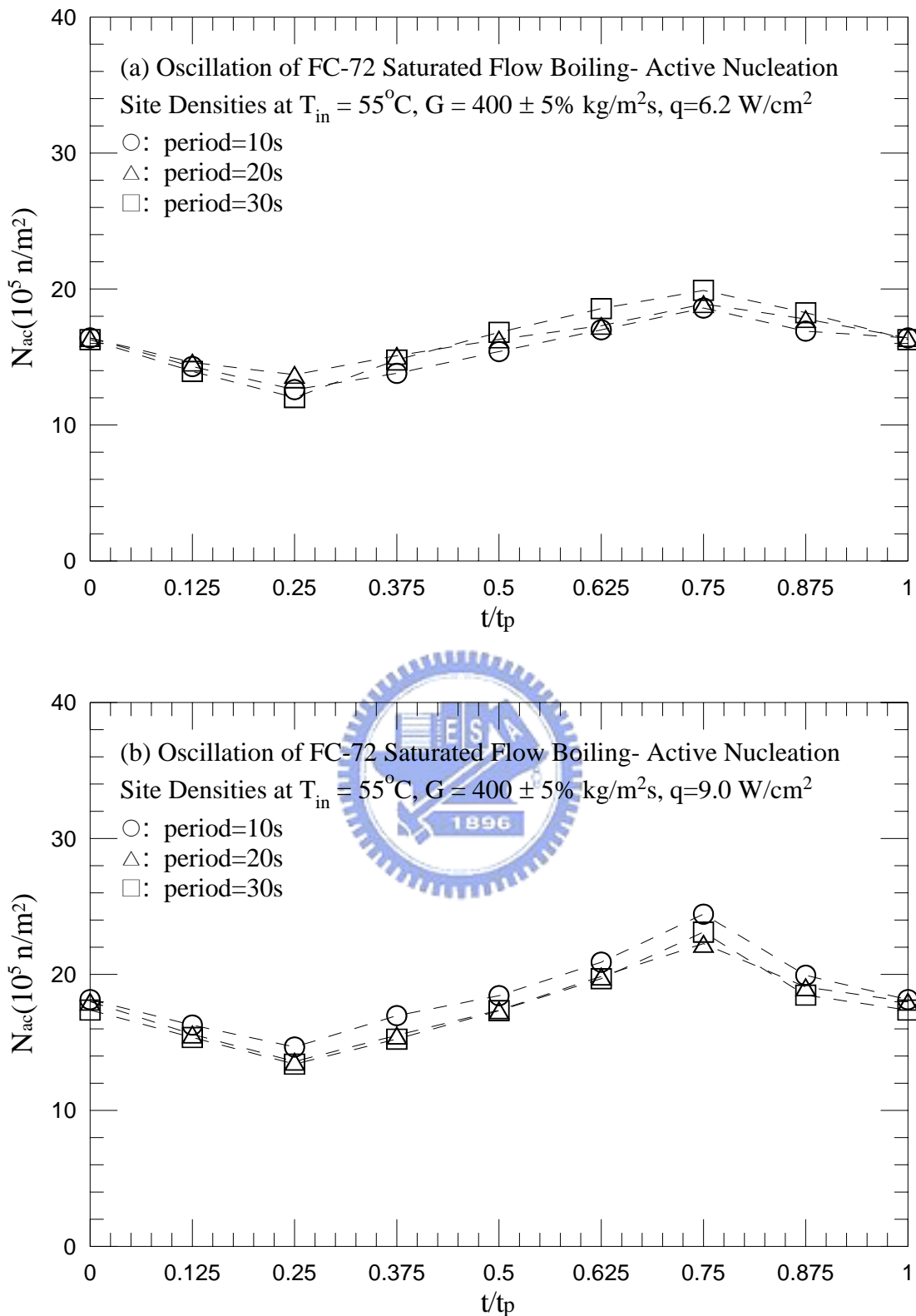


Fig. 4.92 Mean active nucleation site densities for various periods of mass flux oscillation for transient saturated flow boiling for  $G=400 \pm 5\% \text{ kg/m}^2\text{s}$  with (a)  $q=6.2 \text{ W/cm}^2$  and (b)  $q=9.0 \text{ W/cm}^2$ .

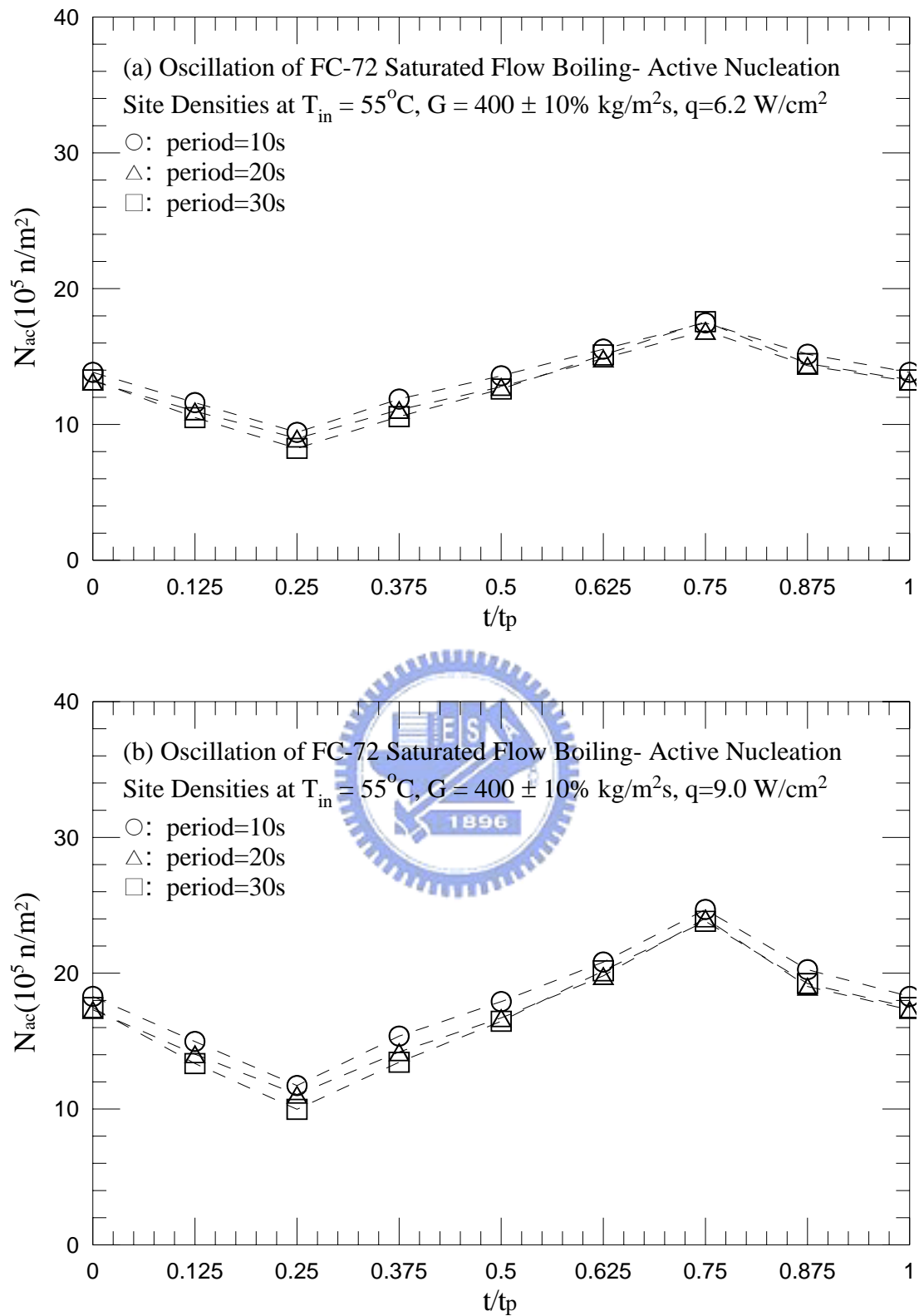


Fig. 4.93 Mean active nucleation site densities for various periods of mass flux oscillation for transient saturated flow boiling for  $G=400\pm10\% \text{ kg/m}^2\text{s}$  with (a)  $q=6.2 \text{ W/cm}^2$  and (b)  $q=9.0 \text{ W/cm}^2$ .

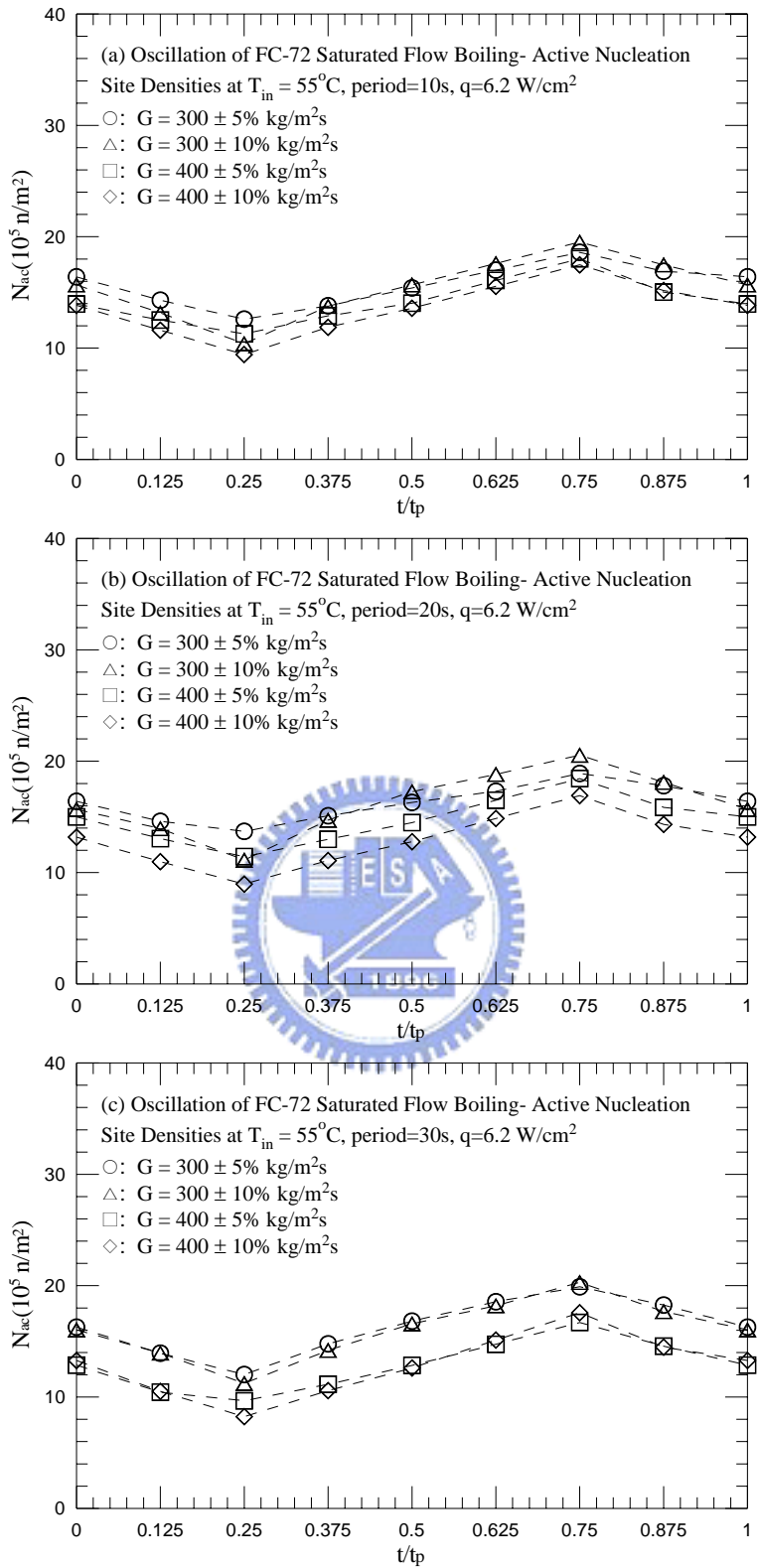


Fig. 4.94 Mean active nucleation site densities for various amplitudes of the mass fluxes oscillation for transient saturated flow boiling for  $q=6.2 \text{ W/cm}^2$  with period=10 sec (a), 20 sec (b), and 30 sec (c).

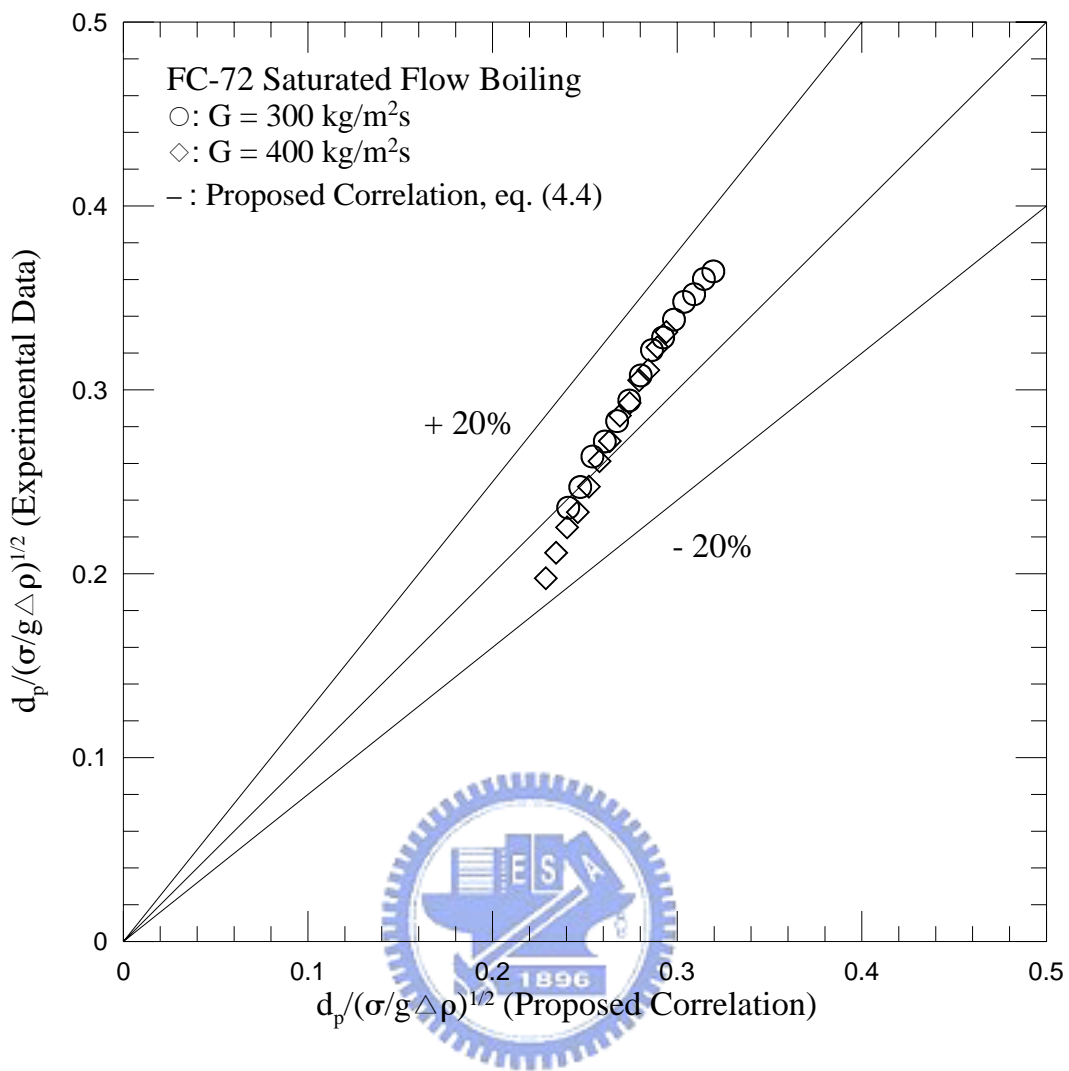


Fig. 4.95 Comparison of the measured data for mean bubble departure diameter for stable saturated flow boiling of FC-72 with the proposed correlation.

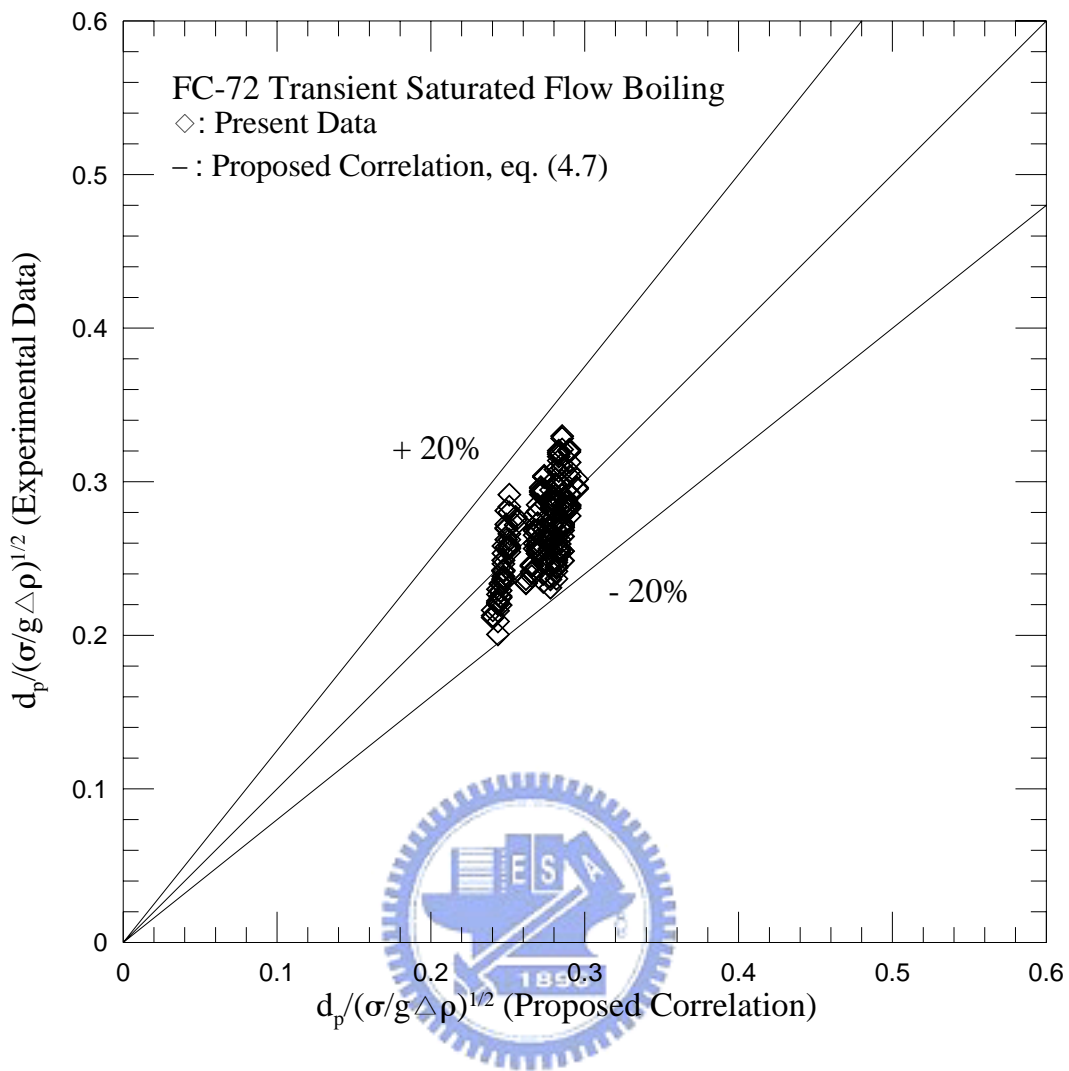


Fig. 4.96 Comparison of the measured data for mean bubble departure diameter for transient saturated flow boiling of FC-72 with the proposed correlation.

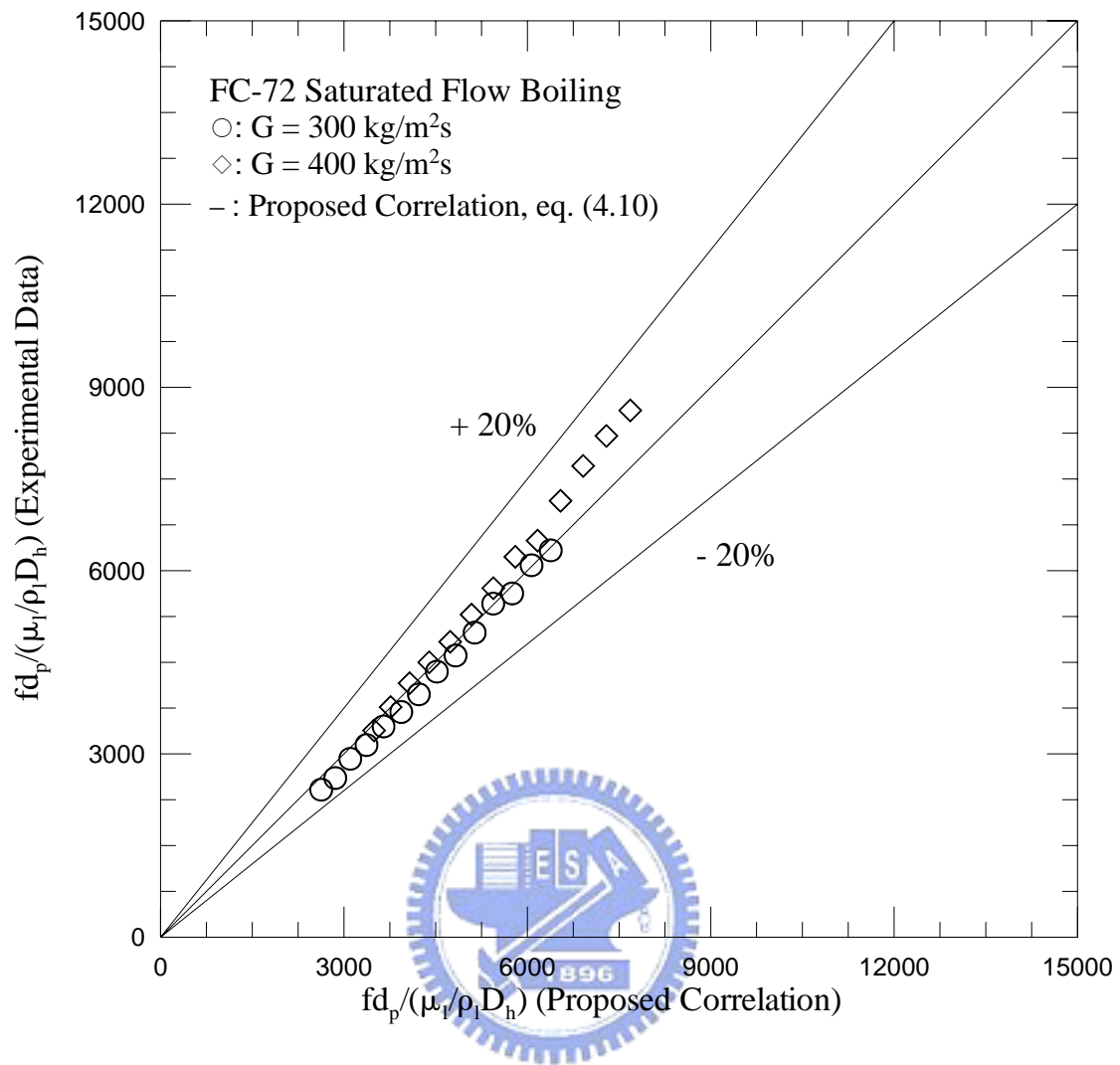


Fig. 4.97 Comparison of the measured data for mean bubble departure frequency for stable saturated flow boiling of FC-72 with the proposed correlation.

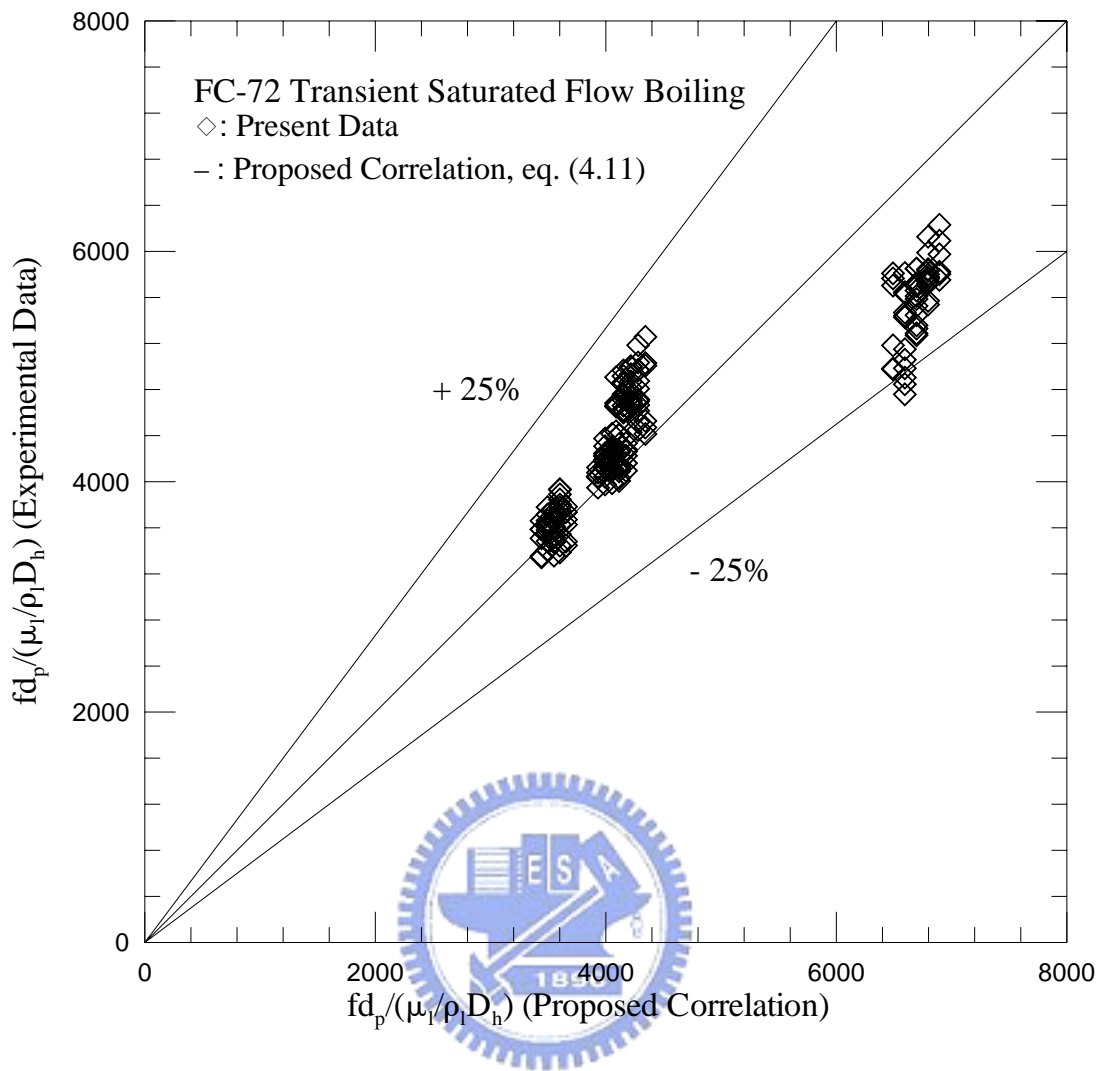


Fig. 4.98 Comparison of the measured data for mean bubble departure frequency for transient saturated flow boiling of FC-72 with the proposed correlation.

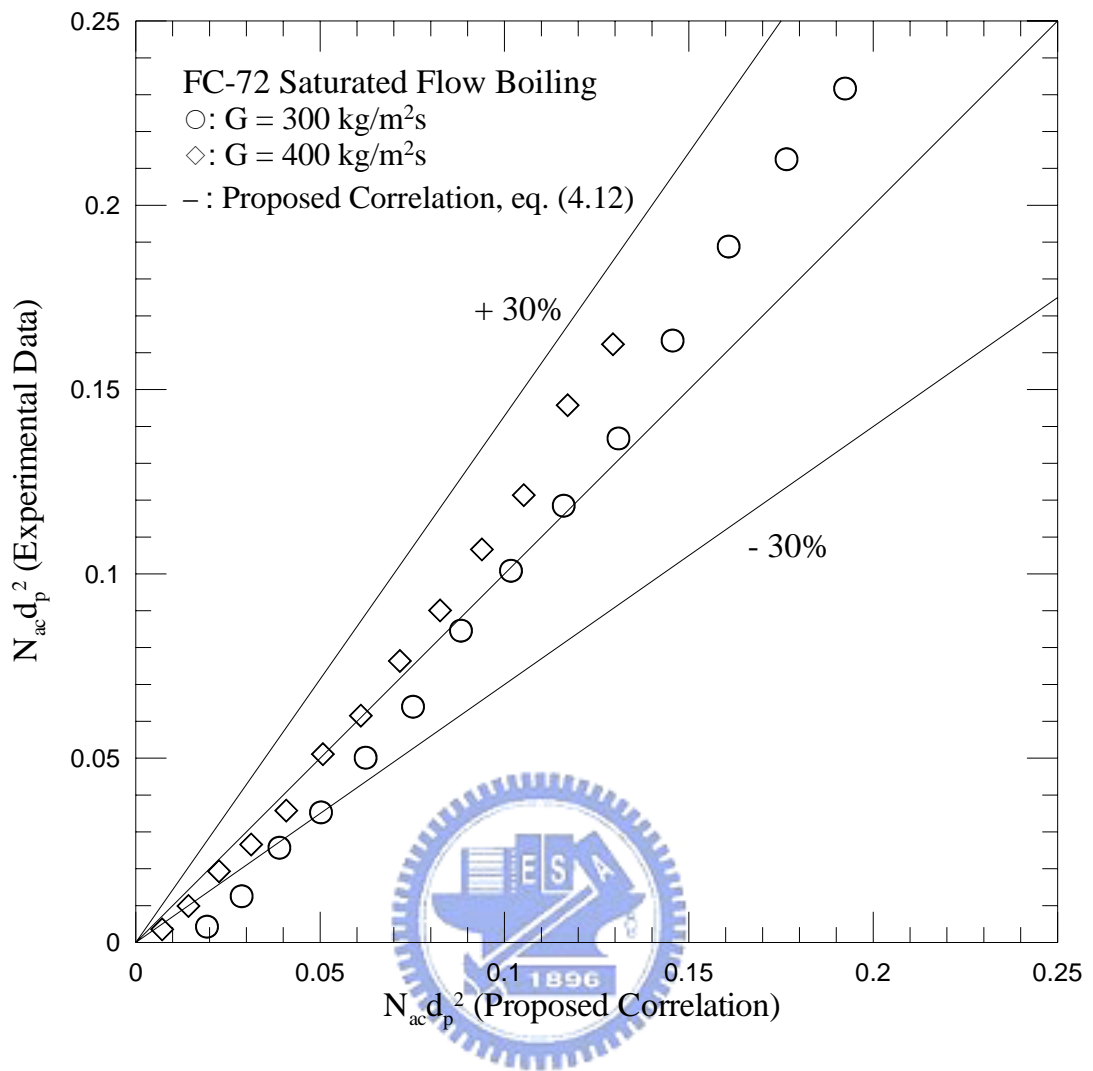


Fig. 4.99 Comparison of the measured data for mean active nucleation site density for stable saturated flow boiling of FC-72 with the proposed correlation.

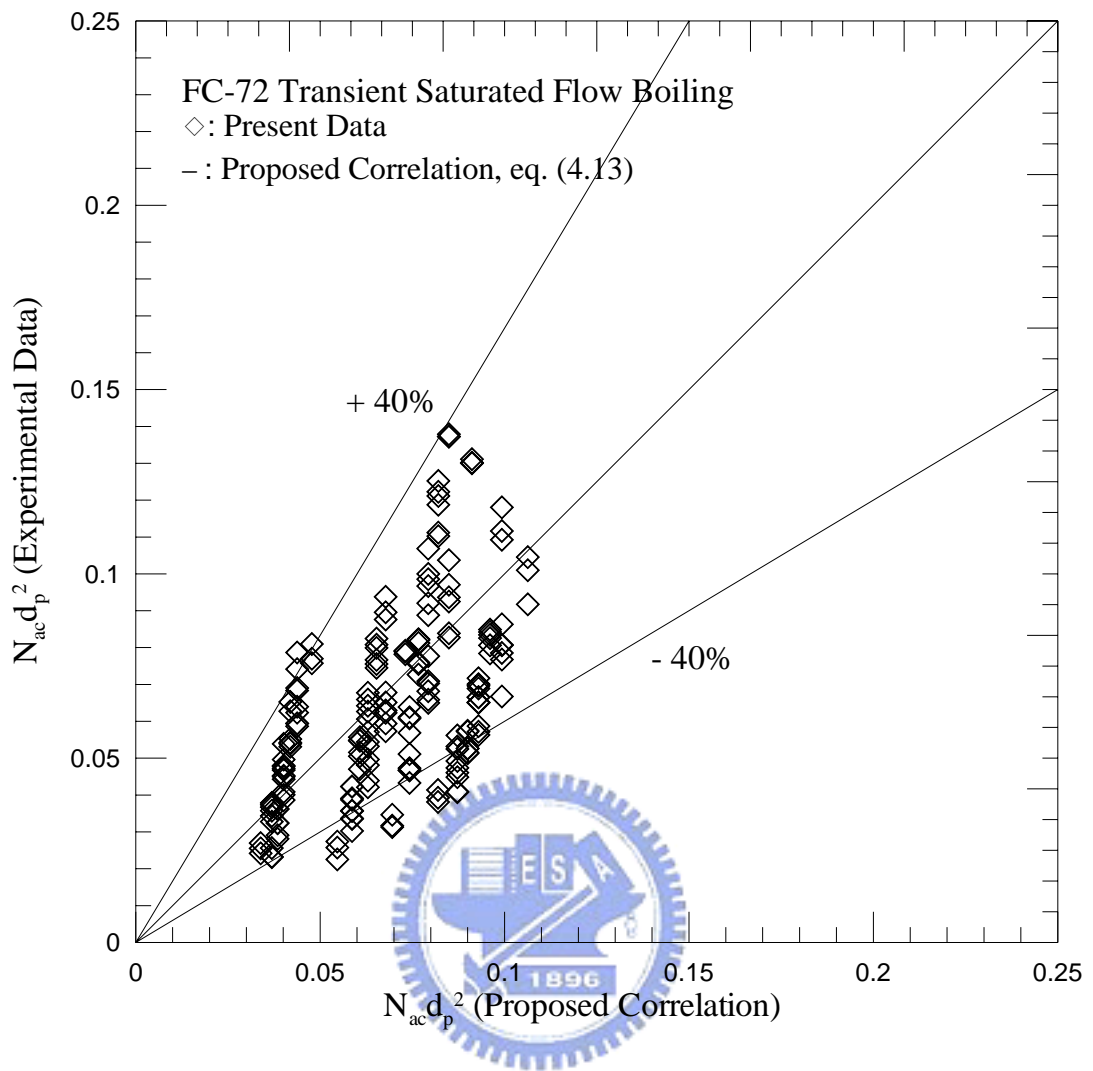


Fig. 4.100 Comparison of the measured data for mean active nucleation site density for transient saturated flow boiling of FC-72 with the proposed correlation.

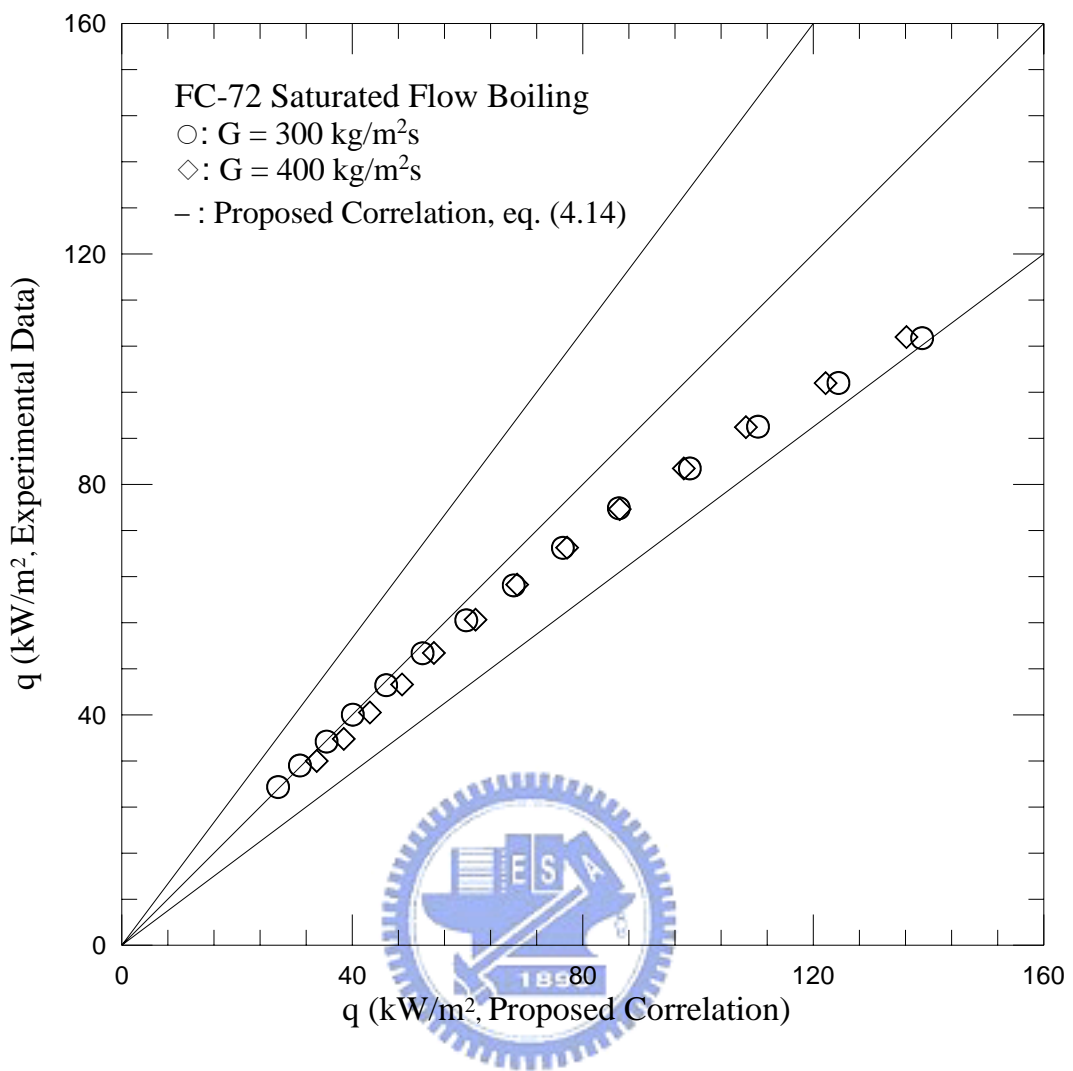


Fig. 4.101 Comparison of the measured data for boiling heat flux for stable saturated flow boiling of FC-72 with the proposed correlation.